# ELECTRODE AND MEMBRANE MODIFICATION OF DIFFERENT REDOX FLOW BATTERIES

A Thesis

Presented to the Faculty of the Graduate School

of Cornell University

In Partial Fulfillment of the Requirements for the Degree of

Master of Science

by

Yiqi Shao

August,2021

## ABSTRACT

The need for the development of effective storage methods for renewably generated electricity has become increasingly evident in the past few decades. With a growing need for the development of large-scale energy storage technologies, the redox flow batteries known for their high capacity, energy efficiency and low cost have attracted huge attention. Among all kinds of different flow batteries, Zinc-based flow batteries (ZBFB) and Vanadium flow batteries (VFB) are two of the most promising system. However, both systems suffer from low reaction rate and high overpotential caused by the low kinetics of 3D current collector as well as the membrane crossover issue. In this thesis, methods of improving electrode interfacial properties and the separator properties were introduced and were applied to both ZBFB and VFB system. Single cell testing, electrochemical measurements and SEM were done to analyze the mechanism behind it.

## BIOGRAPHICAL SKETCH

Yiqi Shao was born in Nanjing China, on December 15, 1995. She developed an interest in chemistry with the guide of her high school chemistry teacher. She was admitted to Sichuan University, as an undergraduate in Polymer Science and Engineering for four years, followed by her MEng at Cornell University. There She join Professor You's group to seek for knowledge on data analysis and machine learning. After graduation, with the interest in battery researches, she joined Joo group as a MS student to carried out independent research in the fascinating field of flow batteries.

## ACKNOWLEDGMENTS

I would like to say thank you to my advisor Professor Yong Lak Joo for including me in the amazing project regarding to flow battery, providing me ideas and helping me with my basic knowledges. I would also like to thank my committee member Professor Jin Suntivich and Professor Alabi for their wonderful suggestions towards my experiments.

I would also like to express my appreciation to my friends Shuo Jin and Xiaosi Gao. They gave me encouragement, help and advice over the whole MS period. Without them, I would definitely be stressed out during my living and studying here.

Finally, I would like to express my gratitude to my parents and the whole Joo group members. It had been a tough year to live and study during the pandemic, the support from my parents and the kindness from my colleagues had made me strong. The time to study with Covid-19 will always be an unforgettable memory for me.

## TABLE OF CONTENT

# CHAPTER 1

# INTRODUCTION

## Flow battery: An Overview

The rapid growth of population and living standard has led to a severe problem on energy storage. With the expectation that fossil fuel will be used up within several centuries, the search for renewable sources has become increasingly urgent.[1,2] To replace the wide-used fossil fuel, renewable energy like solar power, hydraulic power, wind power and temporary electrical storage have been developing rapidly in recent years and is attracting wide attention.[3] However, these renewable sources have a nature of intermittent, the weather not predictable and sunlight do not guarantee either, all these problems can lead to difference of generation of power day-to-day. As one of the solutions of this problem, the concept of flow battery is involved. Generated from the design of fuel cells, a typical flow battery contents a flow cell, two electrolyte tank and a pump.[4] Electrochemical reactants are content in the tank outside of the cell, they will be pumped into the electrode where the reaction is happening. A separator inside divides the cell into anode part and cathode part and it also works as a pathway of conductive ions (Figure 1.1).[5]

The flow batteries are specially designed for large facilities in the first place. One of the most attractive point for flow battery is the scalability and feasibility.[6,7] With tanks containing electroactive material, the flow battery be designed to almost all kinds of scales to meet need for different industry need. However, with the advantages like high energy efficiency, high capacity, low cost and safety, people begin to apply it

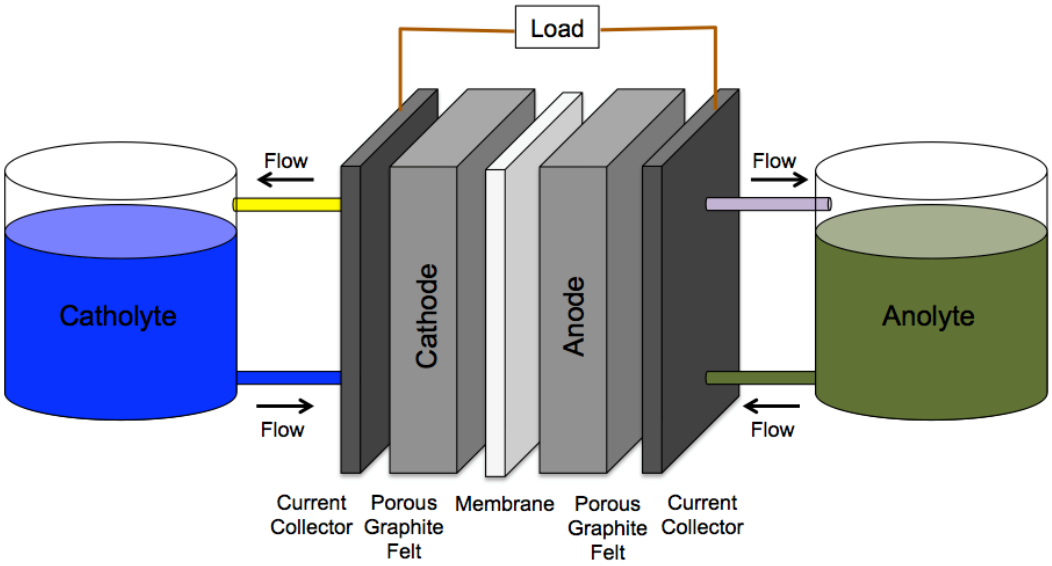


**Figure 1.1. Schematic of a typical redox flow battery.**

to other smaller devices, like electric cars, soft robots and so on. Still, the nature of low voltage and low energy density has limited its use in electronic devices.[8] Normally, the Li ion battery used for phones are smaller enough with a voltage of 3.7V while for the most mature flow battery: vanadium redox flow battery, the voltage is only 1.25V with complicated system and large size.[9–11] Although flow battery technology still has a long way to go, it still has great potential as a replacement for fossil fuels.

***References***

1. Turner, J. A. A Realizable Renewable Energy Future. 285, 687–690 (1999).

2. Yang, Z. et al. Electrochemical Energy Storage for Green Grid. 3577–3613 (2011).

3. Dunn, B., Kamath, H. & Tarascon, J. M. Electrical energy storage for the grid: A battery of choices. Science (80-. ). 334, 928–935 (2011).

4. Wang, W. et al. Recent progress in redox flow battery research and development. Adv. Funct. Mater. 23, 970–986 (2013).

5. Shah, A. B., Zhou, X., Brezovec, P., Markiewicz, D. & Joo, Y. L. Conductive Membrane Coatings for High-Rate Vanadium Redox Flow Batteries. ACS Omega 3, 1856–1863 (2018).

6. Yue, M. et al. Flow field design and optimization of high power density vanadium flow batteries: A novel trapezoid flow battery. AIChE J. 64, 782–795 (2018).

7. Zhang, H. Progress and perspectives of flow battery technologies. Curr. Opin. Electrochem. 18, 123–125 (2019).

8. Leung, P. K., Ponce-De-León, C., Low, C. T. J., Shah, A. A. & Walsh, F. C. Characterization of a zinc-cerium flow battery. J. Power Sources 196, 5174–5185 (2011).

9. Tarascon, J. M. Key challenges in future Li-battery research. Philos. Trans. R. Soc. A Math. Phys. Eng. Sci. 368, 3227–3241 (2010).

10. Skyllas-Kazacos, M., Chakrabarti, M. H., Hajimolana, S. A., Mjalli, F. S. & Saleem, M. Progress in Flow Battery Research and Development. J. Electrochem. Soc. 158, R55 (2011).

11. Ding, C., Zhang, H., Li, X., Liu, T. & Xing, F. Vanadium flow battery for energy storage: Prospects and challenges. J. Phys. Chem. Lett. 4, 1281–1294 (2013).

# CHAPTER 2

# DIRECT ADDITION OF THE NITROGEN AND SULFUR FUNCTIONAL GROUPS IN ELECTRODE OF VANADIUM REDOX FLOW BATTERIES TO ACHIEVE CATALYTIC EFFECT

**Keywords:** Vanadium redox flow Batteries, Energy storage, Sulfate, Amine, Catalyst

**Highlights:**

- Achieved doping of functional groups to graphite felt using a simple way of hydrothermal treatment.
- Largely enhanced the efficiency and the reversibility for the Vanadium flow battery system.

## ABSTRACT

Vanadium redox flow battery is a widely used type of flow battery. It has attracted widespread attention due to its high energy efficiency, good reversibility, high capacity and low cost. Despite such advantages, the Vanadium flow battery design has been largely limited by its high overpotential caused by the low reaction rate. In this chapter, we attempt to use a simple way of hydrothermal treatment to dope catalytic functional groups like Sulfonic and Nitrogen groups onto various kinds of electrodes. Doping Catalytic groups leads to lower overpotential and better cycling performance while the great wettability enhancement result in the improvement of energy efficiency. We also proposed the catalytic mechanism based on the current data.

## 1. INRODUCTION

As the development of economy and living standard improve, the demand of energy keeps increasing. The need for clean, cheap and efficient renewable energy has gone up drastically.[1,2] To replace the wide-used fossil fuel, renewable energy like solar power, hydraulic power, wind power and temporary electrical storage have been developing rapidly in recent years and is attracting wide attention.[3] As a large-scale energy storage technique, flow batteries play a key role in large facilities and the backup energy system.[4,5] There are a variety of flow batteries, but among all these types, the vanadium flow battery (VFB) is known to be the most promising system.[6,7] With the huge advantages like safety, high energy efficiency, ability to work under high current density and also relatively high working voltage, VFB stands out from all types of different flow batteries and is currently being commercialized.[8,9]

A VFB normally utilizes four oxidation states of vanadium: V(II) and V(III) as anolyte, V(IV) and V(V) as catholyte. A V(IV) salt will be dissolved into a supporting acid and transfers to different valences by charging. Normally, these two couples can yield a promising cell voltage of around 1.25V when fully charged.[10] To be specifically:

Anolyte reaction:

$$V^{3+}{}_{(aq)} + e^- \leftrightarrow V^{2+}{}_{(aq)} \qquad E = -0.255V \text{ vs. SHE}$$

Catholyte reaction:

$$[VO_2]^+{}_{(aq)} + 2H^+ + e^- \leftrightarrow [VO]^{2+}{}_{(aq)} + H_2O \qquad E = 1.00V \text{ vs. SHE}$$

Still, the overpotential caused by low kinetics and reaction rate has limited the application of VFB in the industry.[11] To solve this problem, ways of electrode

modification are proposed. Among all these methods, carbon materials are most widely-used.[12] In 2008, H.Q. Zhu proposed a graphite-carbon nanotube composite for electrodes for VFB, with the good electrochemical properties of CNT, the electrode obtained good kinetics and yielded nice performance.[13] While in 2013, applying electrospun carbon nanofibers to the graphite surface, this carbon nanofibers with diameter of 100-200 nm could largely change the surface conductivity and add more reaction sites to the surface.[14]

Nitrogen doped materials begin to be utilized since 2016 when L. Wu doped N-doped nanospheres as electrocatalyst to graphite and achieved a high current density of 100 $mA/cm^2$.[15] In addition to the carbon materials, some metal catalysts like Copper, Nickel, Bismuth and so on are also being considered.[15–18] In 2016, L. Wei published a paper on Applied Energy proposing a newly designed system using copper nanoparticles to be deposited onto the graphite surface. This nanoparticle showed great electrocatalytic properties leading to high capacity under high current density.[15]

Above applications have mostly stick to doping particles onto the current collector surface, in the meantime, people begin to add functional groups onto the electrode.[19–21] The method can add catalysts while change the surface wettability which is one of the most importance factor on changing reaction kinetics of flow battery. Hydroxy groups are the most popular types, because of its hydrophilicity and active nature.[22,23] People utilize the etching method of KOH[23,24], copper[25], $KMnO_4$[26,27] and other oxidative solution to dope hydroxy groups. In the meantime, Nitrogen groups are also considered,[28–30] the most wide-used salt utilized to add functional groups is the

ammonia hydroxide.[29] While in 2018, Dr. Andrew Shah from our group applied ammonia persulfate (APS) for the first time to add sulfonic groups as well as amino group.[31,32] He tried to prove the catalytic effect of these functional groups and achieve high performance even under a high current density of 200 mA/cm$^2$.

In this chapter, we will try to repeat Dr. Shah's work in new graphite felts and apply this method to special graphite felts from our collaborator: StorEn.

## 2. EXPERIMENTAL METHODS

### 2.1 Electrode preparation

One set of samples was hydrothermal treated by Ammonium persulfate (APS). APS was dissolved into 100 mL DI water with different concentration of 0.1M, 0.2M, 0.3M. Different kinds of pristine graphite felt (GF) (PAN-based, AVCarb 101 and StorEn) were submerged into this solution, which was then placed into a Teflon-lined hydrothermal reactor. After that, it was heated in an air furnace at 180℃ for 15 hours and cold down for 10 hours. Then, the GF was washed thoroughly by DI water for 5 minutes to remove the residual. Another set of samples was air-thermal treated under 420°C for 10 hours in the air furnace, and cools down under normal temperature for 5 hours.

### 2.2 Single cell testing

In the single cell testing, the flow battery consists of a cell, a pump and two glass containers to hold the electrolyte. The Vanadium electrolyte was pumped into the flow cell through ¼" I.D. tubing (Tygon 2375 Ultra tubing) using a mechanical pump (Masterflex L/S Digital Drive, 600 rpm, 15/230 VAC). The structure of the flow cell

was quite complicated. There were a pair of acrylic or metal end plate working as the shell of the cell, two Viton rubber gaskets to make sure the sealing, two graphite current collectors, two HDPE plastic gaskets to control the compressing rate and two 3D printed PE flow frames. A pre-treated separator which was Nafion 212 in this case, would then be added to avoid possible electrolyte crossover. Each side of the cell had a 1 to 2 mm space between the membrane and current collector, in which a piece of 3 mm thick, 3 cm wide and 5 cm long porous graphite felt (PAN-based, AVCarb and StorEn) was compressed to reach good electrical contact. The electrolyte was 25 mL 1M $VOSO_4$ in 4M $H_2SO_4$ for Anode side and 50 mL of the same electrolyte for cathode side. Each container was purged of Argon for 2 minutes to get rid of Oxygen which would be harmful for the cycling process. Since the effective chemical V(V) and V(II) are extremely unstable and expensive, we decide to prepare them in a flow cell by the charging process of V(IV). To accomplish a maximum conversion from V(IV) to V(V) and V(II), we intend to use an upper cut off voltage of 1.7 V under a constant current density of 15 $mA/cm^2$ and repeat the cycle for 5 times under Argon atmosphere. The color of V(V) and V(II) should be yellow and purple, the appearance of these two colors showed a full conversion of the electrolyte. After the full conversion, 25 mL of the extra catholyte should be taken out in order to maintain the mass balance, the electrolyte volume applied was 25 mL for both catholyte and anolyte, with a flow rate of 30 mL/min and current density of 50 $mA/cm^2$ which was 750 mA in this case. The upper cutoff voltage was 1.7 V while the lower cutoff voltage was set to 0.8 V according to the reduction potential. The rate capability was also tested, the current density ranged

from 50 mA/cm$^2$ to 200 mA/cm$^2$. All the single cell testing was carried out with a battery analyzer from MTI (3A, 5V).

### 2.3 Materials Characterization

Both air treated and APS treated graphite felts were characterized by different kinds of analytical techniques. The XPS was used to examine the elements on the surface and their quantity. Raman spectroscopy (Renishaw InVia Confocal Raman microscope, 785nm laser) was applied to detect the carbon crystallinity and morphology. SEM (Zeiss Gemini 500 Scanning Electron Microscope) was used to observe the structure of the carbon fiber in order to eliminate the structural factor and prove the structural integrity. EDS together with the SEM was done to further examine the element on the fiber surface. The water contact angle (VCA Optima Contact Angle) was tested to figure out the wettability changes on the surface.

## 3. RESULTS AND DISCUSSION

The goal of the treatment was to come up with a simple and effective method to permanently add catalytic functional groups onto the graphite felt (GF) electrodes. In the meantime, the sulfonic groups and hydroxy groups were theorized to be hydrophilic groups which would improve the GF kinetics and the flow performance as well. The data of this chapter was mainly divided into 2 parts, in the first part we tried to apply Andrew's method to new type of GF and proved the feasibility of this method to be tried in other electrodes. In the second part, we applied this method to StorEn company's sample.

This proposed treatment uses an inexpensive and efficient oxidant known as ammonia persulfate (APS). It has high water solubility and the persulfates can decompose to form reactive free radicals. Therefore, the sulfonic groups would then be linked to the carbon and added to the surface of GF. Before the single cell testing, several characterizations were done to explore the properties of both air-treated and APS-treated GF. SEM images were displayed below in the Figure 3.1. We could figure out that all the GF had

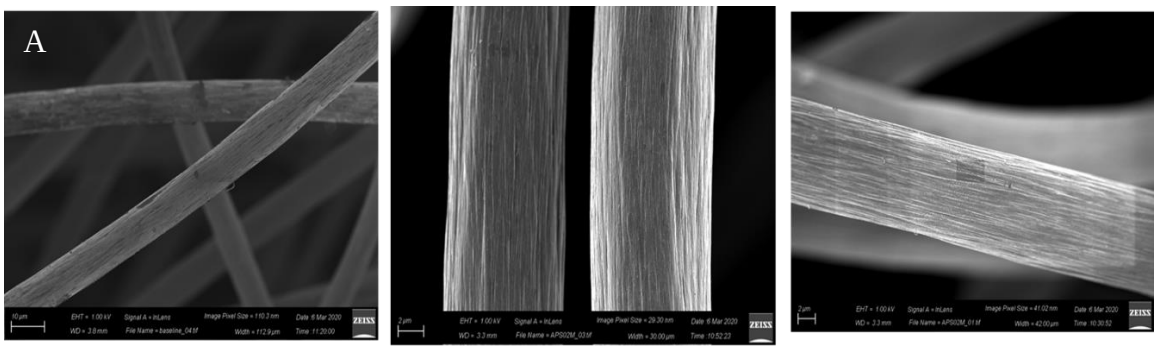


**Figure 3.1. SEM images of (A) GF (B) Air-treated GF (C) APS treated GF.**

no obvious difference, indicating both air treatment and APS could maintain a great structural integrity. The water contact angle was tested to analyze the hydrophilicity (Figure 3.2). The Figure 3.2A was for control group, Figure 3.2B was for air treated one

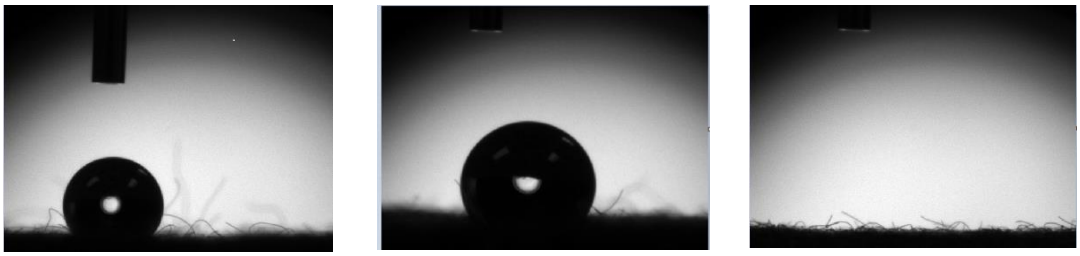

**Figure 3.2. Water contact angle images of (A) GF, 115.04° (B) Air-treated GF, 101.79 ° (C) APS treated, no angle.**

while the Figure 3.2C was from APS treated one. It was clear that the baseline and air-treated one was quite identical with only 14° difference in angle (115.04 ° for baseline,

101.79 ° for air treatment). However, the APS treated case, the water contact angle was too small to be detected. This showed a great improvement in surface wettability by adding functional groups with APS and also indirectly proved the successful addition of hydrophilic groups. Further characterization like XPS was completed to detect bonds and analyze groups, showed in Figure 3.3 and Table 3.1. Red line represented the air-treated case, we could see that there was only small difference of about 2% in oxygen element while the blue line for APS treatment, we could see S groups being added to the surface together with more oxygen element. The Nitrogen element had also been proven to be added though the amount was quite low, only about 0.55%. Therefore,

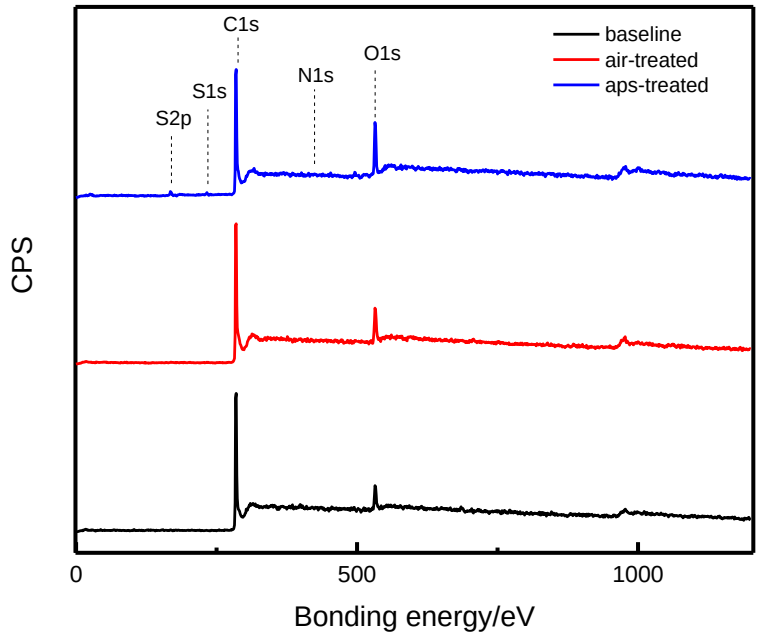


**Figure 3.3. XPS plot of control group, air-treated GF and APS treated GF.**

**Table 3.1. Element percentage of different GF.**

| At% | C | O | S | N |
|---|---|---|---|---|

| | | | | |
|---|---|---|---|---|
| GF | 93.43% | 6.57% | 0 | 0 |
| Air-treated | 90.83% | 8.32% | 0 | 0 |
| APS-treated | 85.55% | 12.39% | 1.51% | 0.55% |

when we tried to analyze the catalytic mechanism the effect of amino group shouldn't be considered too much. Single cell testing was completed using different APS treatment of different concentration, the results were showed in Figure 3.4 to Figure 3.6.

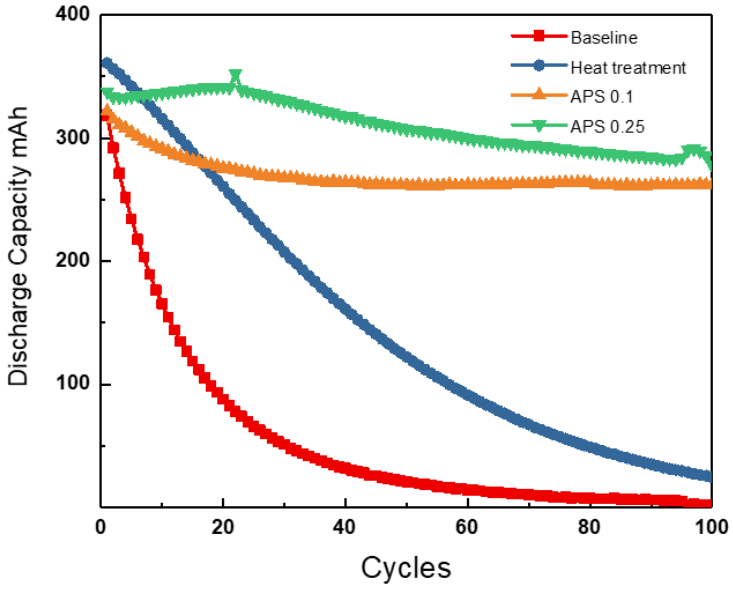


**Figure 3.4. Comparison of cycling results using control group, air treatment, APS treatment with different concentrations under a current density of 50 mA/cm$^2$.**

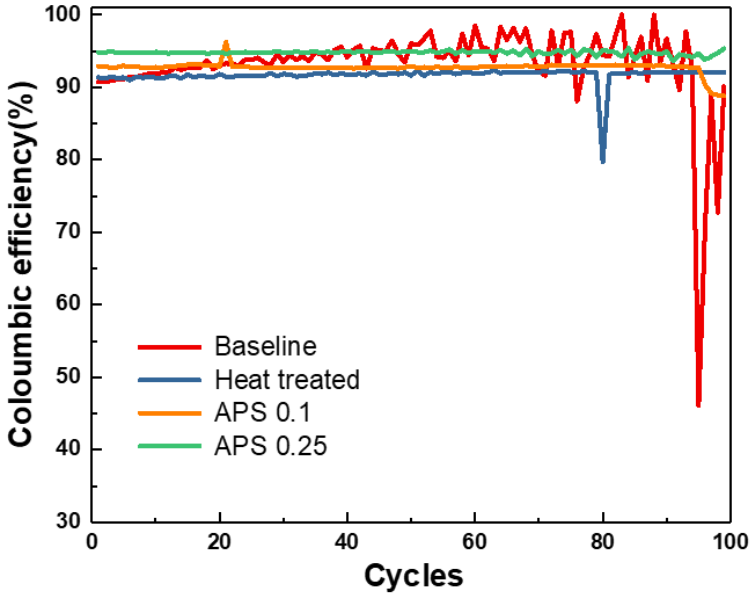


**Figure 3.5. Comparison of Coulombic efficiency results for different treated GF.**

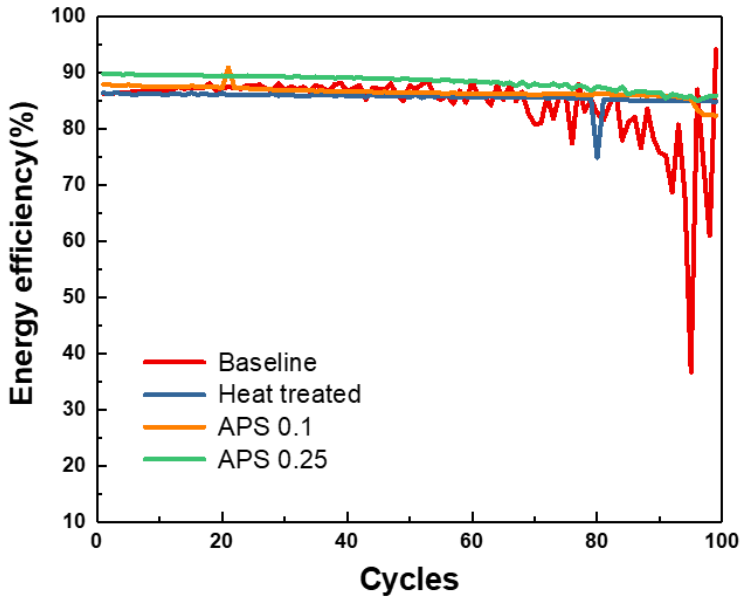


**Figure 3.6. Comparison of Energy efficiency of different treated GF.**

These 3 figures presented the discharge capacity, coulombic efficiency and energy efficiency under current density of 50 mA/cm$^2$. The discharge capacity was the most obvious one, we could see a rapid drop of baseline and air treated one, however, the APS treated one showed a much more promising reversibility. They maintained a

capacity of around 300 mAh even after 100 cycles. The Figure 3.5 presented the coulombic efficiency and Figure 3.6 showed the energy efficiency. Both efficiency for the control and air-treated case was not good, the fluctuating data indicated that the battery was died at that time. However, the CE for APS treated one stabilized at 91% to 93% and the EE to around 90%. The great performance of CE indicated the good kinetics and better electrochemical activity of the treated GF, while the better EE demonstrated lower overpotential which indicated higher reaction rate. In these 3 figures, concentration of APS solution was also discussed. It was reported that the 0.25M had relatively best performance in all three aspects. This threshold of concentration might generate from the conductivity change. The more sulfonic groups added the less conductive it would be, therefore catalytic effect and conductivity issue met with balance leading to this threshold.

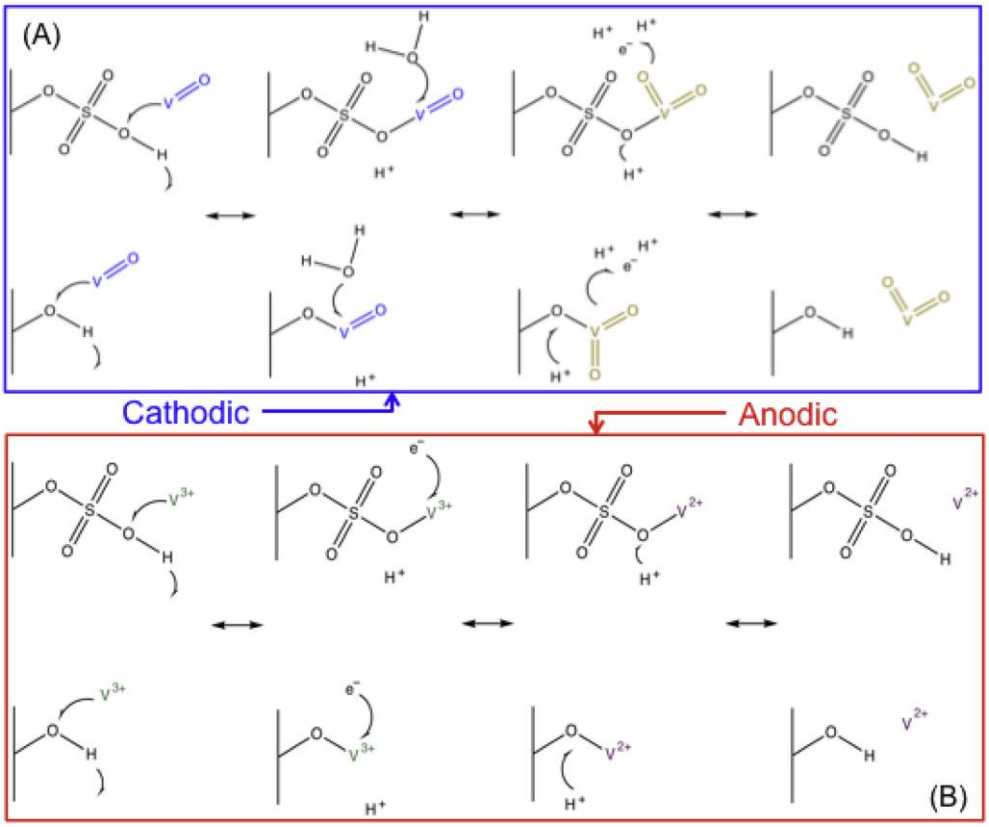

**Figure 3.7. Proposed catalytic mechanism of APS treated GF with functional groups of amino group, sulfonic group and hydroxy group.**

Based on the fact that APS doping was successful and effective. A proposed catalytic mechanism was put forward. During the oxidative charging process in the catholyte, the oxygen or nitrogen groups in the surface would act as initial reaction sites for the $VO^{2+}$ ion to temporarily bond, displacing a proton. Oxygen from water in the electrolyte would bond to vanadium complex, generating two additional protons and an electron, forming $VO_2^+$. In the anolyte, the $V^{3+}$ could displaced a proton then bonded with an oxygen from the functional group, forming an intermediate complex. An electron could then be taken away from the graphite felt, subsequently releasing the vanadium ion, which was then transferred into the $V^{2+}$ state. (Figure 3.7)

This method was subsequently utilized to StorEn's GF. There was huge property difference between two kinds of GFs. It was obvious from Figure 3.8 that the StorEn GF was no comparable to the commercialized one. It had over 15% of decrease of capacity, 10% lower of CE and 7% decline in EE. The main reason for that came from

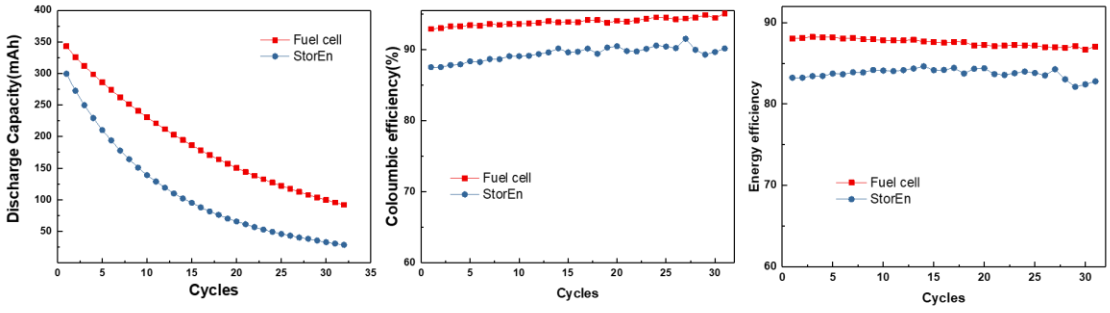


**Figure 3.8. Discharge capacity, coulombic efficiency and energy efficiency comparison of Fuel cell store GF and GF from StorEn under current density of 50 mA/cm$^2$.**

impurity. After comparing the EDS figure of control group of commercialized GF and

StorEn GF, we found out there was some S element in StorEn's sample (Figure 3.9, 3.10).

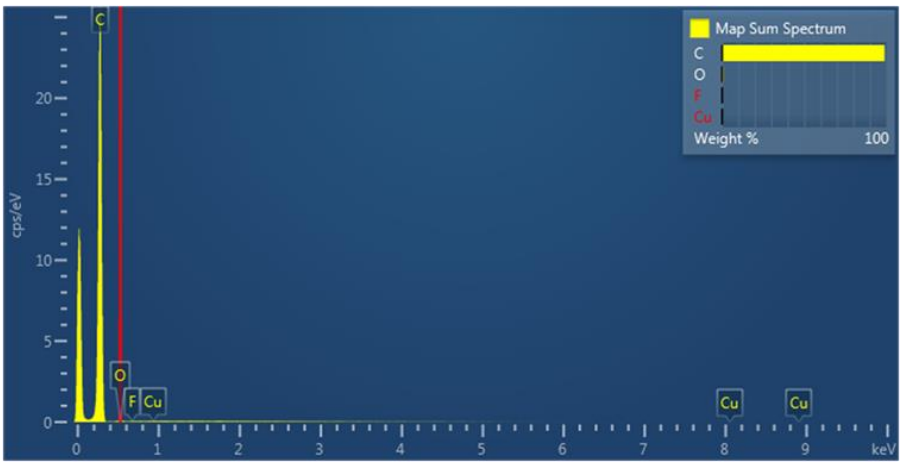


**Figure 3.9. The EDS image of Fuel cell store GF**

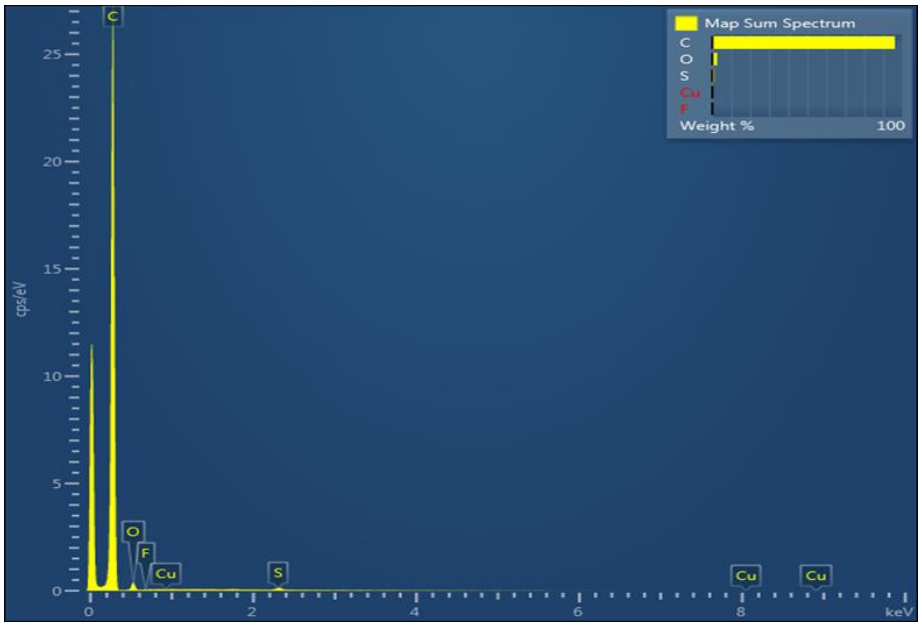


**Figure 3.10 The EDS image of StorEn GF.**

Even with this difference, the result of APS treatment was still satisfied. Displayed in Figure 3.11, we could see a big difference in reversibility, EE as well as the discharging

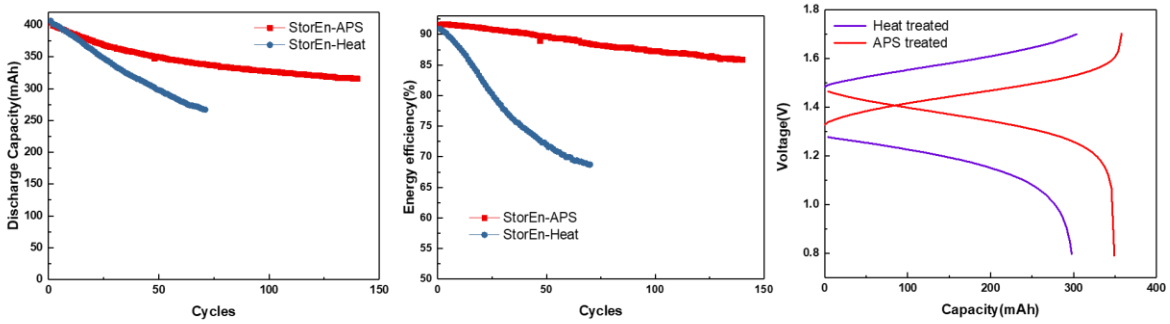


**Figure 3.11. (A) Discharge capacity, (B) energy efficiency and (C) capacity-voltage curve comparison of APS treated StorEn felts and Air treated StorEn felts.**

voltage presented in Figure 3.11C. Optimized APS concentration for StorEn's GF was 0.2 M which was different from Fuel cell one. The threshold of APS concentration might be the result of competence between catalytic effect of functional groups and the conductive decrease due to addition of sulfonic groups. Finally, rate capability was tested and displayed here as Figure 3.12 to Figure 3.14. The Current density ranged from 50 mA/cm$^2$ to 200 mA/cm$^2$. (50-75-100-125-150-175-200-50). The APS treating one performed much better than the baseline under high current density. The better

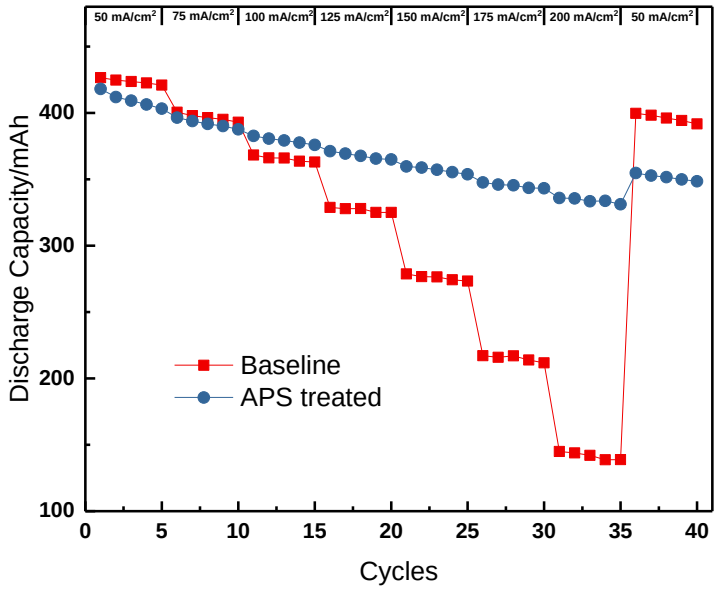

**Figure 3.12. Rate capability of comparison of discharge capacity between control group and APS treated one under current density between 50 to 200 mA/cm$^2$.**

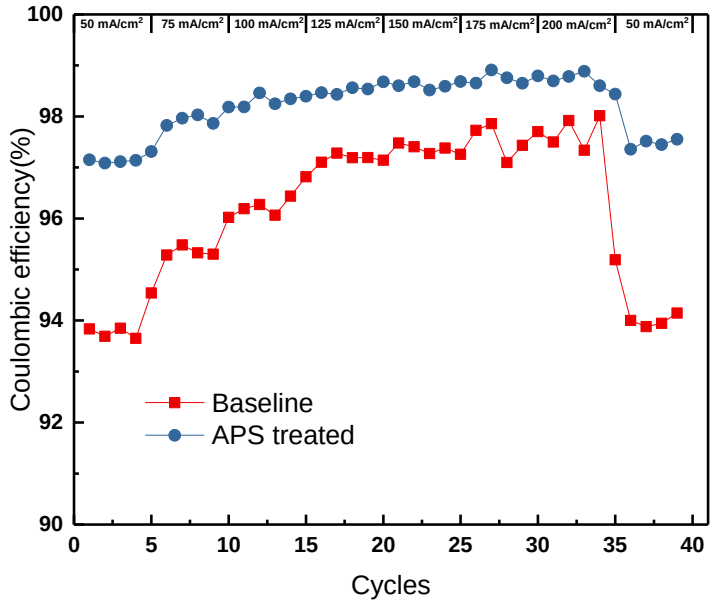


**Figure 3.13. Rate capability of comparison of coulombic efficiency between control group and APS treated one under current density between 50 to 200 mA/cm2.**

performance of baseline under low current density was probably the result of error of volume of electrolyte. APS had obvious effect on both CE and EE which again proved our assumption of increase of electrode kinetics and decrease of overpotential.

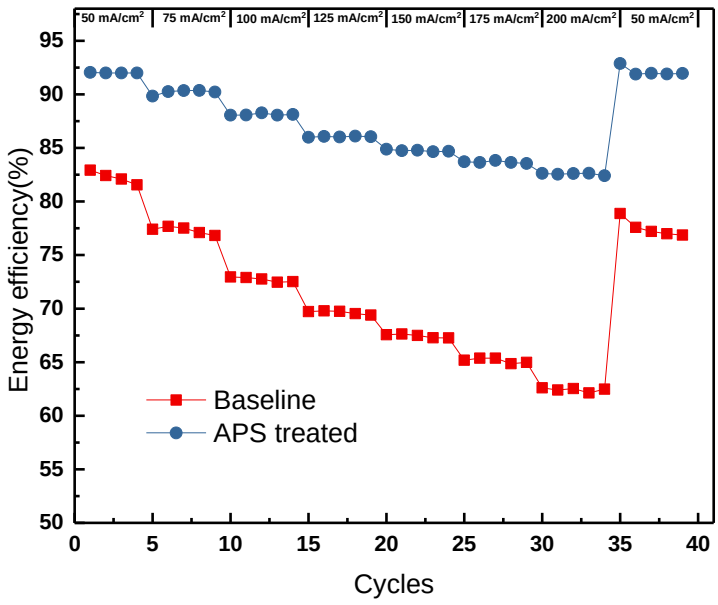


**Figure 3.14. Rate capability of comparison of energy efficiency between control group and APS treated one under current density between 50 to 200 mA/cm2.**

## 4. CONCLUSION

We successfully repeated the data of Dr Shah and applied this method to another kind of electrode. Then we proved the addition and catalytic effect of functional groups, discussed the electrode kinetics change. We also discovered threshold of APS concentration and tried to discuss the reason. The wettability improvement of GF was as well, one of the most important factors in our treatment, this enhancement helped to improve flow performance as well as energy efficiency. Finally, we utilized Dr. Shah's method to StorEn's GF and enhanced the overall performance. The rate capacity showed the consistency of improvement even under high current density.

***Reference***


1. Turner, J. A. A Realizable Renewable Energy Future. **285**, 687–690 (1999).
2. Yang, Z. *et al.* Electrochemical Energy Storage for Green Grid. 3577–3613 (2011).
3. Dunn, B., Kamath, H. & Tarascon, J. M. Electrical energy storage for the grid: A battery of choices. *Science (80-. ).* **334**, 928–935 (2011).
4. Wang, W. *et al.* Recent progress in redox flow battery research and development. *Adv. Funct. Mater.* **23**, 970–986 (2013).
5. Zhang, H. Progress and perspectives of flow battery technologies. *Curr. Opin. Electrochem.* **18**, 123–125 (2019).
6. Rychcik, M. & Skyllas-Kazacos, M. Characteristics of a new all-vanadium redox flow battery. *J. Power Sources* **22**, 59–67 (1988).
7. Skyllas-Kazacos, M., Chakrabarti, M. H., Hajimolana, S. A., Mjalli, F. S. & Saleem, M. Progress in Flow Battery Research and Development. *J. Electrochem. Soc.* **158**, R55 (2011).
8. Yue, M. *et al.* Flow field design and optimization of high power density vanadium flow batteries: A novel trapezoid flow battery. *AIChE J.* **64**, 782–795 (2018).
9. Zhao, P. *et al.* Characteristics and performance of 10 kW class all-vanadium redox-flow battery stack. *J. Power Sources* **162**, 1416–1420 (2006).
10. Shah, A. A., Watt-Smith, M. J. & Walsh, F. C. A dynamic performance model for redox-flow batteries involving soluble species. *Electrochim. Acta* **53**, 8087–

8100 (2008).

11. Kim, K. J. *et al.* A technology review of electrodes and reaction mechanisms in vanadium redox flow batteries. *J. Mater. Chem. A* **3**, 16913–16933 (2015).
12. Chakrabarti, M. H. *et al.* Application of carbon materials in redox flow batteries. *J. Power Sources* **253**, 150–166 (2014).
13. Zhu, H. Q. *et al.* Graphite – carbon nanotube composite electrodes for all vanadium redox flow battery. **184**, 637–640 (2008).
14. Wei, G., Liu, J., Zhao, H. & Yan, C. Electrospun carbon nano fi bres as electrode materials toward 2 redox couple for vanadium fl ow battery. *J. Power Sources* **241**, 709–717 (2013).
15. Wei, L., Zhao, T. S., Zeng, L., Zhou, X. L. & Zeng, Y. K. Copper nanoparticle-deposited graphite felt electrodes for all vanadium redox flow batteries. *Appl. Energy* **180**, 386–391 (2016).
16. Busacca, C. *et al.* High performance electrospun nickel manganite on carbon nanofibers electrode for vanadium redox flow battery. *Electrochim. Acta* **355**, (2020).
17. Blasi, A. Di, Busacca, C., Blasi, O. Di, Briguglio, N. & Antonucci, V. Synthesis and Characterization of Electrospun Nickel-Carbon Nanofibers as Electrodes for Vanadium Redox Flow Battery. *J. Electrochem. Soc.* **165**, A1478–A1485 (2018).
18. Li, B. *et al.* Bismuth nanoparticle decorating graphite felt as a high-performance electrode for an all-vanadium redox flow battery. *Nano Lett.* **13**,

1330–1335 (2013).

19. Sun, B. Modification of Graphite Electrode Materials. *Electrochim. Acta* **37**, 1253–1260 (1992).

20. Zhang, W. *et al.* Electrochemical activation of graphite felt electrode for VO 2+/VO2+ redox couple application. *Electrochim. Acta* **89**, 429–435 (2013).

21. Noh, C., Moon, S., Chung, Y. & Kwon, Y. Chelating functional group attached to carbon nanotubes prepared for performance enhancement of vanadium redox flow battery. *J. Mater. Chem. A* **5**, 21334–21342 (2017).

22. Wei, Y. & Jia, C. Q. Intrinsic wettability of graphitic carbon. *Carbon N. Y.* **87**, 10–17 (2015).

23. Jiang, Y. *et al.* Fungi-Derived, Functionalized, and Wettability-Improved Porous Carbon Materials: An Excellent Electrocatalyst toward VO 2+ /VO 2 + Redox Reaction for Vanadium Redox Flow Battery . *J. Electrochem. Soc.* **165**, A1813–A1821 (2018).

24. Zhang, Z., Xi, J., Zhou, H. & Qiu, X. Electrochimica Acta KOH etched graphite felt with improved wettability and activity for vanadium fl ow batteries. **218**, 15–23 (2016).

25. Zhou, X., Zhang, X., Lv, Y., Lin, L. & Wu, Q. Nano-catalytic layer engraved carbon felt via copper oxide etching for vanadium redox fl ow batteries. *Carbon N. Y.* **153**, 674–681 (2019).

26. Jiang, H. R., Shyy, W., Ren, Y. X., Zhang, R. H. & Zhao, T. S. A room-temperature activated graphite felt as the cost-e ff ective , highly active and

stable electrode for vanadium redox fl ow batteries. *Appl. Energy* **233**–**234**, 544–553 (2019).

27. Hassan, A. & Tzedakis, T. Facile chemical activation of graphite felt by KMnO4 acidic solution for vanadium redox flow batteries. *Appl. Surf. Sci.* **528**, 146808 (2020).

28. Park, S. & Kim, H. Fabrication of nitrogen-doped graphite felts as positive electrodes using polypyrrole as a coating agent in vanadium redox fl ow batteries †. 12276–12283 (2015).

29. Wu, T. *et al.* Hydrothermal ammoniated treatment of PAN-graphite felt for vanadium redox flow battery. *J. Solid State Electrochem.* **16**, 579–585 (2012).

30. Wu, L., Shen, Y., Yu, L., Xi, J. & Qiu, X. Boosting vanadium flow battery performance by Nitrogen-doped carbon nanospheres electrocatalyst. *Nano Energy* **28**, 19–28 (2016).

31. Shah, A. B., Wu, Y. & Joo, Y. L. Direct addition of sulfur and nitrogen functional groups to graphite felt electrodes for improving all-vanadium redox flow battery performance. *Electrochim. Acta* **297**, 905–915 (2019).

32. Figueiredo, J. L. & Pereira, M. F. R. The role of surface chemistry in catalysis with carbons. *Catal. Today* **150**, 2–7 (2010).

# CHAPTER 3

# CONDUCTIVE MEMBRANE COATING FOR HIGH PERFORMANCE VANADIUM REDOX FLOW BATTERY

**Keywords:** Vanadium redox flow Batteries, Energy storage, Carbon nanotube, Graphene, Air-controlled electrospray

**Highlights:**

- Applied electrospray technique to dope carbon material on the separator surface.
- Largely enhanced the reversibility of the Vanadium flow battery system.
- Improved the cell electrical conductivity thus reduced the surface resistance.

## ABSTRACT

Vanadium redox flow battery is the only type of flow battery that has been well commercialized. It has attracted widespread attention due to its outstanding performance as a large-scale energy storage. Despite various kinds of advantages, the Vanadium flow battery performance has been largely limited by the huge problem of membrane crossover and its high cell resistance. In this chapter, we attempt to use electrospray to dope carbon ink containing CNT or graphene to reduce the cell electrical resistance. In the meantime, the ink will work as a protection to the separator and decrease the crossover.

## 1. INRODUCTION

As the development of economy and living standard improve, the demand of energy keeps increasing. The need for clean, cheap and efficient renewable energy has gone up drastically.[1–3] To replace the widely-used fossil fuel, renewable energy like solar power, hydraulic power, wind power and temporary electrical storage have been developing rapidly in recent years and is attracting wide attention.[4–6] As a large-scale energy storage technique, flow batteries play a key role in large facilities and the backup energy system. There are a variety of flow batteries, but among all these types, the vanadium flow battery (VFB) is known to be the most promising system.[7,8] With the huge advantages like safety, high energy efficiency, ability to work under high current density and also relatively high working voltage, VFB stands out from all types of different flow batteries and is currently being commercialized.[9–12]

Still, VFB possess many issues to be solved. One of the most urgent one is the separator crossover.[13,14] Rooted from the design of fuel cells,[7,15] flow batteries use the same type of proton exchange membrane: Nafion created from DuPont company. Nafion separators mainly consist of tetrafluoroethylene backbone (PTFE) with perfluorovinyl ether groups terminated with sulfonate groups.[16] With this component, Nafion possesses high mechanical property, good chemical resistance and good ion conductivity.[17] The use of Nafion as the separator started since the born of vanadium flow battery. During the reaction, the hydrogen ions are transferred from one side to the other making the cell a close circuit. However, during the charge and discharge process, V(II) and V(III) in the anode side with smaller molecular size will also diffuse to the

cathode, the phenomena is regarded as crossover. Since V(II) and V(III) are reactants, the crossover will cause self-discharge leading to a big drop to the capacity.[14,18]

Numerous ways are introduced to solve this problem. The most popular one is to replace Nafion. Although Nafion has great property, its huge cost has limited the use of flow battery in the industry. Among all those replacements, cross-linked sulfonated poly (ether ether ketones) known as SPEEK is the most promising one.[19] The use SPEEK is also generated from fuel cell application. In 2011, Zhensheng Mai first involved the SPEEK to the VFB system,[19] and in 2014 a graphene/SPEEK membrane was introduced to public by Wenjing Dai and achieved great electrochemical property and reversibility.[20,21] Other concepts like making modification to Nafion are also quite popular. In 2008, Qingtao Luo came up with an idea to apply Polyethylenimine (PEI) to the surface of Nafion and changed the permeation of relevant vanadium ion.[22] However, this change led to an increase of the resistance. In the same year, Franck Pereira reported a method by impregnation with Ionic liquids. Silica nanoparticles were also introduced to Nafion in order to improve the electrochemical property.[23] And in 2018, Dr. Shah from our group proposed a method to electrospray CNT onto the surface, improved the electric conductivity and helped change the permeability in the meantime.[24,25] Electrospray is a method which adds an electric field to force liquid particles to move forward. These particles will then be collected by a conductivity substrate, in this case 3D electrode and then stick to it. This a cheap and mature technique to be applied in the battery field.

In this chapter, we applied Dr. Shah's method to our collaborator Ashawn's membrane,

trying to further prove the feasibility of his method and apply other materials like graphene to reduce the cost.

## 2. EXPERIMENTAL METHODS

### 2.1 Ink preparation

The conductive ink consisted of Carbon materials, Nafion dispersion (20 wt%, Ion power) and DI water. We tried 2 different kinds of Carbon materials: Carbon nanotube (CNT) and graphene. The CNT were highly conductive material which would largely increase the conductive of the system. However, since the CNT was a 3D tubing structure, the price was not comparable to the 2D structure materials like graphene. Therefore, 2D graphene materials were also tried in this project. The composition of ink can be a key factor to the electrospray, the well-dispersed solution can help form the layer on the surface and improve the ability to control the solution amount. After several trying, the best receipt for CNT ink was: 1.5 wt% CNT, 20 wt% Nafion dispersion, and 78.5 wt% DI water. The solution with this amount of CNT was neither too dilute nor too concentrated. However, for the graphene solution, we followed a receipt from the electrode modification which I would cover later in this thesis: 4 wt% Graphene, 2 wt% Nafion dispersion, 92 wt% DI water.

### 2.2 Electrospray

The Carbon ink was ultrasonicated for 1 to 1.5 hours before use in order to maintain the well-dispersed situation. The solution was then switched to a 5 mL syringe and a needle with tube gauge of 10 and shell gauge of 17. Ten psig of air was applied through the shell of the needle while the pump (Harvard Apparatus) pushing the syringe to spray

the solution out. Both the Nafion 212 and the Ashawn membrane were dried and bundled with a copper mesh. The copper mesh consisted of several 1 mm square holes which would prevent the ink fully covering the surface and lead to blocking holes and bad ion conductivity. The membranes were then placed on a current collector at a distance of 15 cm from the tip of the needle. The positive lead was connected to the end of the needle while the other side to the current collector and the voltage was set to 25 kV. (Figure 2.2.1) The flow rate would vary from different amount of solution, it was found that if the ink would form a disperse surface if we limit the spraying to 3 minutes for CNT and 4 minutes for graphene. The solvent evaporation rates would be properly balanced by the deposition while in the meantime, the speed was not too low to get the ink particle through mesh. Both sides of the separator were sprayed in every case with different loading of 0.030 mg CNT/ $cm^2$, 0.025 mg CNT/$cm^2$, 0.025mg/$cm^2$ graphene.

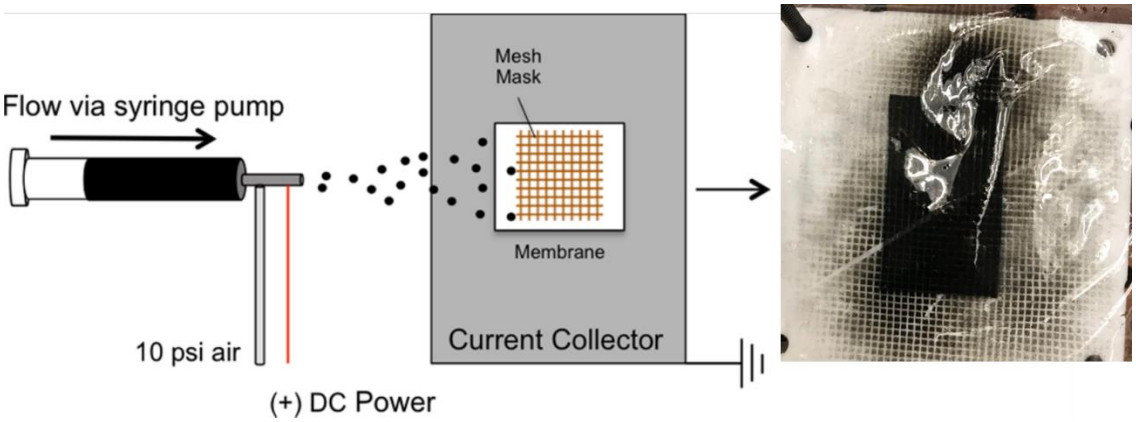


**Figure 2.2.1 Schematics of electrospray.**

### 2.3 Single cell testing

In the single cell testing, all other settings were the same to the previous chapter except the use of Carbon treated Ashawn and Carbon treated Nafion membrane. The electrode were air-treated PAN-based graphite felt with AVCarb. The electrolyte volume used

was 25 mL for both sides, with the same flow rate of 30 mL/min and current density of 50 mA/cm$^2$ which was 750 mA. All the membrane would be water treated for at least 12 hours to enhance the ion conductivity and maintain the mechanical property.

### 2.4 Materials Characterization

SEM (Zeiss Gemini 500 Scanning Electron Microscope) was used to observe the structure of the carbon fiber in order to eliminate the structural factor and prove the structural integrity. EDS together with the SEM was done to further examine the element on the fiber surface.

## 3. RESULTS AND DISCUSSION

The previous goal for this chapter was to improve the system electric conductivity by doping carbon materials onto the Nafion separator surface. However, with deeper understanding of vanadium flow battery, we have figured out the key point for this system: Crossover. Although spraying carbon onto separator surface did improve the electric conductivity of system, this change might not have noticeable effect since the membrane only played a key role on ion transfer. Therefore, the main reason for this treatment had changed to reduce crossover effect without damaging the ion conductivity of Nafion. We utilized two carbon materials: carbon nanotubes and graphene to two types of membranes: Nafion and Ashawn's membrane.

The Figure 3.1 showed the macro-morphology of the carbon materials on the surface. We could see small carbon cubes caused by the copper mesh which would reduce the resistance increase of separator. SEM images were taken to have a clear view of micro-morphology of carbon materials. Figure 3.2 was the SEM photo for graphene on the

Ashawn's membrane surface. Due to low conductivity of substrate, these images were

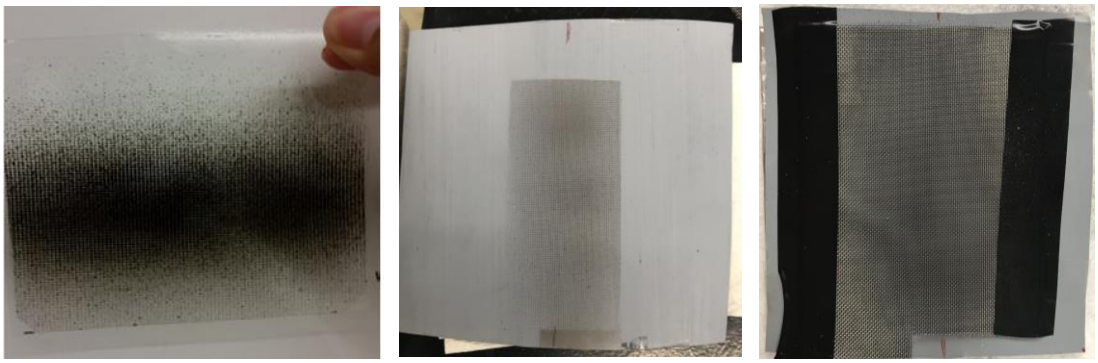

**Figure 3.1. Images for carbon-electrosprayed separators (A) CNT on Nafion (B) Gr on Ashawn (C) CNT on Ashawn using copper mesh.**

not clear enough to show the whole view of carbon distribution. However, under higher scale, the graphene characteristic could easily be detected. In Figure 3.2B under 100 μm scale, we could see graphene evenly distributed on the surface, while in Figure 3.2C

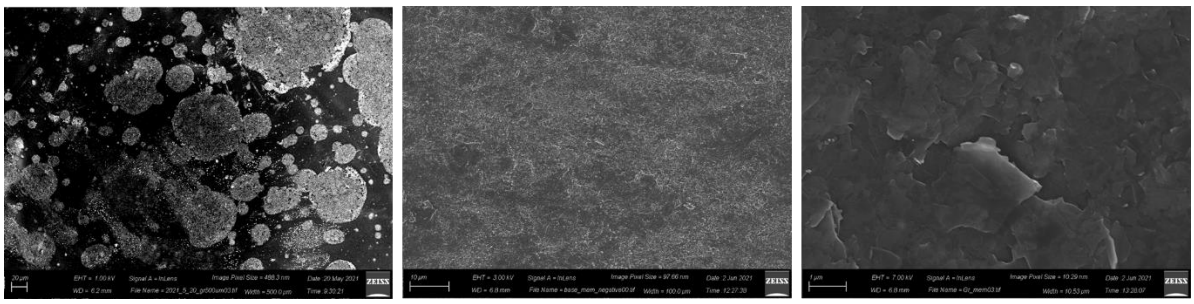

**Figure 3.2 SEM images for Gr on Ashawn. (A) 400μm scale (B) 100μm scale (C) 10μm scale.**

under even lower scale of 10 μm, the special layer by layer structure of graphene could be detected. The SEM images for CNT treatment was displayed in the Figure 3.3 below.

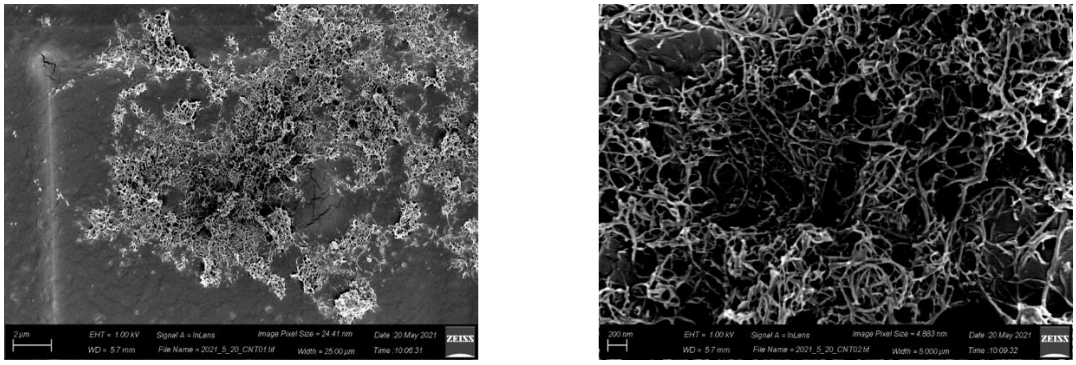

**Figure 3.3. SEM images for CNT on Ashawn. (A) 25μm scale (B) 5μm scale.**

Compared to the graphene case, we could figure out the tubing structure which made the carbon layer into 3D. Although it had been less even for CNT case, its higher conductivity and better 3D structure would lead to better surface contact with electrode and resulted in lower resistance. In the meantime, the tubing structure is giving some small holes for the water to move inside.

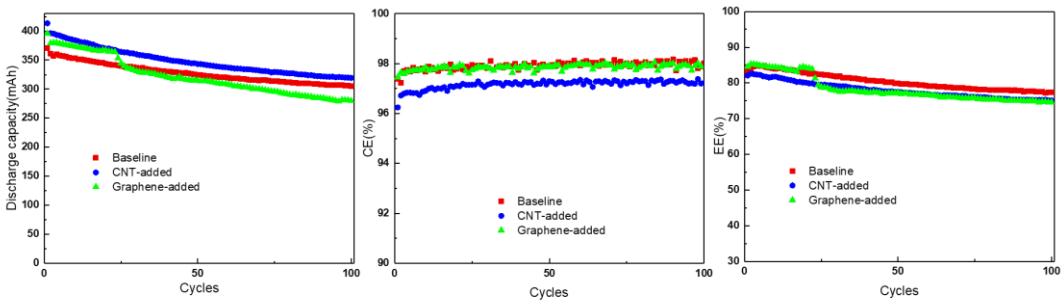


**Figure 3.4. Single testing for Nafion, CNT doped Nafion and Gr doped Nafion. (A) Discharge capacity (B) Coulombic efficiency (C) Energy efficiency.**

The single cell testing was then completed, from the Figure 3.4 we could tell that the CNT doped cell could have an 8.3% of capacity increase while the graphene one performed similar and drop rapidly after a few cycles. This indicated the advantages of 3D structure of CNT which provide holes for water to get contact with the Nafion inside. However, CNT case didn't come out with good result in CE and EE, main reason for

this might as well relate to ion conductivity. When we involved the carbon layer to treat the surface, we would inevitably reduce the ion conductivity but this would also lead to better anti-crossover ability which significantly increased the capacity. The graphene case had similar CE and EE as the control possibly due to low amount and even distribution. Since the flat structure caused contact issues, the discharge capacity was not comparable to the improvement of CNT case.

After that, we applied this method to Ashawn's membrane. The results were presented as Figure 3.5. We had a 28% of increase on capacity after 100 cycles. Although the CE has a 1% decrease, the EE increases for 6% indicating that the overpotential has been

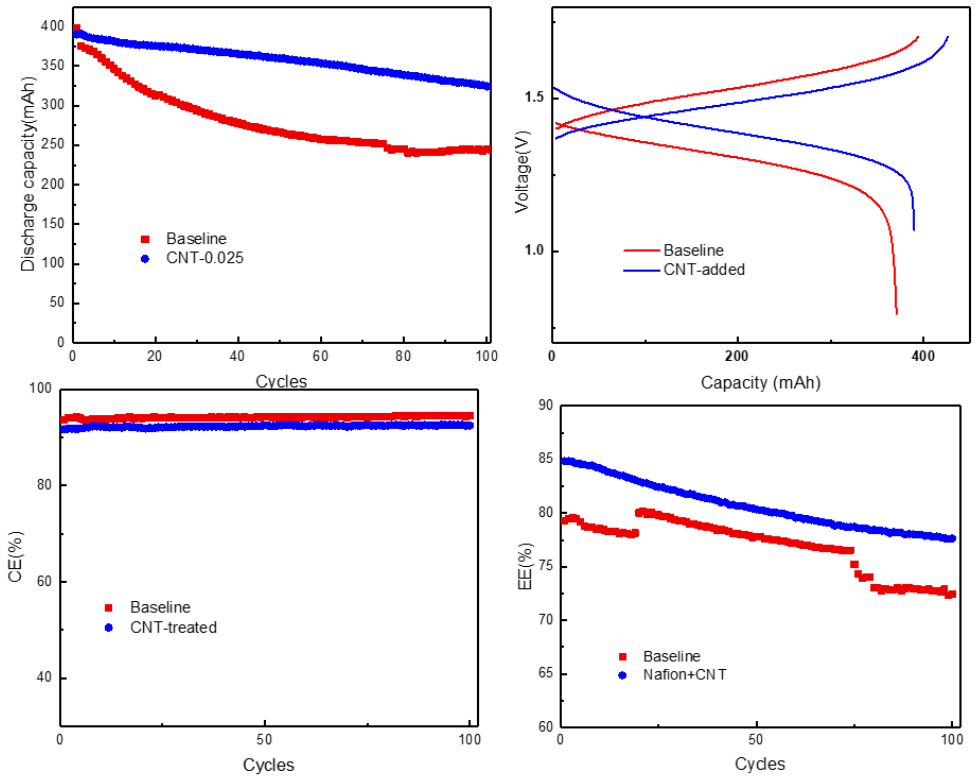


**Figure 3.5 Single cell testing for Ashawn and CNT-doped Ashawn. (A) Discharge capacity (B) Capacity-voltage curve. (C) Coulombic efficiency. (D) Energy efficiency.**

reduced and the system conductivity is higher than the baseline. The decrease has CE

may relate to the decrease of diffusion coefficient caused by CNT doping, this problem may be solved by improved skills and spray method. This was a surprising result since the quality of Ashawn's membrane had bad shape and nature. Their membrane's ability to prevent crossover was extremely weak, even causing Osmosis effect due to crossover of V(II) and V(III). However, with the use of our treatment, this effect was largely inhibited. The graphene case was also tried for Ashawn's separators (Figure 3.6). When changing from CNT to GR, although we could see an improve of CE and EE, the discharge capacity didn't improve that much. The reason for that was discussed previously: The structure of CNT and GR was different. CNT was in 3D while graphene was known as 2D materials. The CNT had 3D tubing structures and the Gr was planar. The Gr might not be flat when being sprayed onto surface, some angle should be expected, and that would lead to bad contact between electrode and membrane while reducing the conductivity.

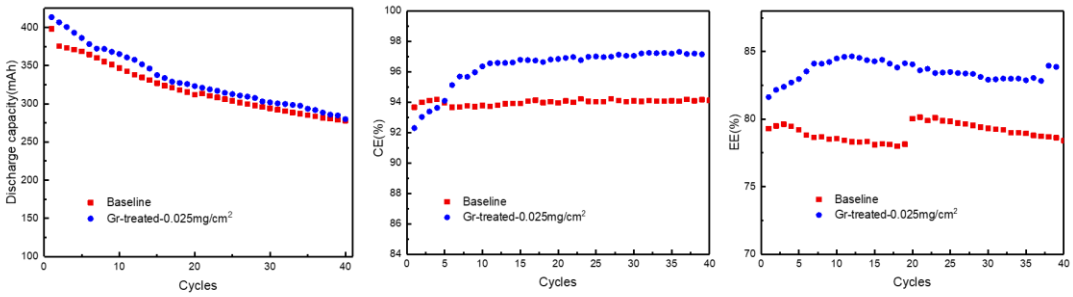


**Figure 3.6. Single cell testing for Ashawn and Gr-doped Ashawn. (A) Discharge capacity (B) Coulombic efficiency. (C) Energy efficiency.**

## 4. CONCLUSION

We successfully sprayed the CNT and Gr onto the membrane surface without largely reducing the ion conductivity of membrane. Also, we proved that this method using

CNT will increase the reversibility, capacity and decrease the overpotential by increasing the electrical conductivity of membrane. The Gr treatment didn't work quite well possibly due to the planar structure of Gr. However we still had a long way to go with this project due to the Ashawn's issue, if the company could provide better samples, better results and deeper study should be expected.

***Reference***


1. Turner, J. A. A Realizable Renewable Energy Future. 285, 687–690 (1999).

2. Yang, Z. et al. Electrochemical Energy Storage for Green Grid. 3577–3613 (2011).

3. Dunn, B., Kamath, H. & Tarascon, J. M. Electrical energy storage for the grid: A battery of choices. Science (80-. ). 334, 928–935 (2011).

4. Wang, W. et al. Recent progress in redox flow battery research and development. Adv. Funct. Mater. 23, 970–986 (2013).

5. Zhang, H. Progress and perspectives of flow battery technologies. Curr. Opin. Electrochem. 18, 123–125 (2019).

6. Rychcik, M. & Skyllas-Kazacos, M. Characteristics of a new all-vanadium redox flow battery. J. Power Sources 22, 59–67 (1988).

7. Skyllas-Kazacos, M., Chakrabarti, M. H., Hajimolana, S. A., Mjalli, F. S. & Saleem, M. Progress in Flow Battery Research and Development. J. Electrochem. Soc. 158, R55 (2011).

8. Parasuraman, A., Lim, T. M., Menictas, C. & Skyllas-Kazacos, M. Review of material research and development for vanadium redox flow battery applications.

Electrochim. Acta 101, 27–40 (2013).

9. Yue, M. et al. Flow field design and optimization of high power density vanadium flow batteries: A novel trapezoid flow battery. AIChE J. 64, 782–795 (2018).

10. Zhao, P. et al. Characteristics and performance of 10 kW class all-vanadium redox-flow battery stack. J. Power Sources 162, 1416–1420 (2006).

11. Rahman, F. & Skyllas-Kazacos, M. Vanadium redox battery: Positive half-cell electrolyte studies. J. Power Sources 189, 1212–1219 (2009).

12. Shah, A. A., Watt-Smith, M. J. & Walsh, F. C. A dynamic performance model for redox-flow batteries involving soluble species. Electrochim. Acta 53, 8087–8100 (2008).

13. Darling, R., Gallagher, K., Xie, W., Su, L. & Brushett, F. Transport Property Requirements for Flow Battery Separators. J. Electrochem. Soc. 163, A5029–A5040 (2016).

14. Vardner, J. T., Ye, A. A., Valdes, D. A. & West, A. C. Current-Driven Vanadium Crossover as a Function of SOC and SOD in the Vanadium Redox Flow Battery. J. Electrochem. Soc. 167, 080512 (2020).

15. Yang, B., Hoober-Burkhardt, L., Wang, F., Surya Prakash, G. K. & Narayanan, S. R. An Inexpensive Aqueous Flow Battery for Large-Scale Electrical Energy Storage Based on Water-Soluble Organic Redox Couples. J. Electrochem. Soc. 161, A1371–A1380 (2014).

16. Prifti, H., Parasuraman, A., Winardi, S., Lim, T. M. & Skyllas-Kazacos, M. Membranes for redox flow battery applications. Membranes (Basel). 2, 275–306 (2012).

17. Mauritz, K. A. & Moore, R. B. State of understanding of Nafion. Chem. Rev. 104, 4535–4585 (2004).

18. Skyllas-Kazacos, M., Cao, L., Kazacos, M., Kausar, N. & Mousa, A. Vanadium Electrolyte Studies for the Vanadium Redox Battery—A Review. ChemSusChem 9, 1521–1543 (2016).

19. Mai, Z., Zhang, H., Li, X., Bi, C. & Dai, H. Sulfonated poly(tetramethydiphenyl ether ether ketone) membranes for vanadium redox flow battery application. J. Power Sources 196, 482–487 (2011).

20. Dai, W. et al. SPEEK/Graphene oxide nanocomposite membranes with superior cyclability for highly efficient vanadium redox flow battery. J. Mater. Chem. A 2, 12423–12432 (2014).

21. Dai, W. et al. Sulfonated Poly(Ether Ether Ketone)/Graphene composite membrane for vanadium redox flow battery. Electrochim. Acta 132, 200–207 (2014).

22. Luo, Q., Zhang, H., Chen, J., Qian, P. & Zhai, Y. Modification of Nafion membrane using interfacial polymerization for vanadium redox flow battery applications. J. Memb. Sci. 311, 98–103 (2008).

23. Pereira, F. et al. Advanced mesostructured hybrid silica-nafion membranes for high-performance PEM fuel cell. Chem. Mater. 20, 1710–1718 (2008).

24. Shah, A. B., Zhou, X., Brezovec, P., Markiewicz, D. & Joo, Y. L. Conductive Membrane Coatings for High-Rate Vanadium Redox Flow Batteries. ACS Omega 3, 1856–1863 (2018).

25. Zhang, L., Zhang, H., Lai, Q., Li, X. & Cheng, Y. Development of carbon coated

membrane for zinc/bromine flow battery with high power density. J. Power Sources 227, 41–47 (2013).

# CHAPTER 4

# ACHIEVING HIGH-PERFORMANCE ZN-$I_2$ FLOW BATTERY BY REGULATING INTERFACIAL PROPERTIES OF 3D CURRENT COLLECTOR

**Keywords:** Zn-$I_2$ Flow Batteries, Energy storage, Graphene, Active Carbon, Air-controlled electrospray, Electrochemical

**Highlights:**

- Applied electrospray technique to dope carbon material on the current collector.
- Largely enhanced the Coulombic efficiency of the Zn-$I_2$ Flow Battery.
- Achieved high performance under high areal capacity and current density.

## ABSTRACT

Zinc-based redox flow battery is one of the best stationary energy storages for large facilities. Its high areal capacity, energy density and low cost have attracted huge attention. However, Zinc-related flow battery has known for its bad reversibility due to severe Zinc dendrite formation. In this chapter, we will try to discuss this problem in the Zinc-$I_2$ system. We successfully resolved this problem by improving interfacial property on current collectors using carbon materials and then examined the mechanism of this enhancement.

## 1. INRODUCTION

As the demand for energy increases, the need for clean, cheap and efficient renewable energy has been increasing drastically.[1–3] Renewable energy like solar power, hydraulic power, wind power and temporary electrical storage have been developing rapidly in recent years and is attracting wide attention.[4,5] Among numerous electrochemical energy storage, the flow batteries (FB) are quite promising due to high safety, high energy efficiency, high flexibility and low cost.[6,7] Researchers have studied numerous kinds of flow battery system since the born of the concept of FB. Vanadium flow battery, Zinc-based flow battery, Iron-chromium flow battery, organic quinone flow battery and even membrane-less flow battery,[7–10] within all these FBs the vanadium flow battery and the zinc-based flow battery are two of most mature systems.[11–13] As a representative type of flow battery technology, the vanadium flow battery (VFB) has been considered as the most practical system and is currently in commercial stage.[12,14] However, the membrane crossover, high cost of vanadium and the low energy density limit its capacity and reversibility.[15,16] With all those huge problems to be solved, people turn their attention to the zinc-based flow battery (ZFB).

Over centuries, numerous ZFBs have been proposed and studied. Zinc-nickel flow battery was reported in 2004 by professor Pletcher, this system was one of the frontier fields at time because of its membrane-less characteristic.[17] In 2011, zinc-cerium flow battery was proposed and studied by Leung et al, it could reach 2.1V at 20 $mA/cm^2$ current density.[18,19] The zinc-iron system was introduced in 2015 by Ke Gong, this system was cheap enough to have $100 per kW h capital cost.[8] However, the most

popular field for ZFB has always been the halogen-zinc system. Charles Renard came up with the zinc-chlorine flow battery system even back to 1884, this study opened the gate for people to explore the use of halogen-zinc system in flow battery.[7] Zinc bromine flow battery, studied by Lim et al. in 1977,[20] was proposed and after 20 years of development, this system has become the most mature system among all the ZFB. While in 2015, the first zinc-iodide flow battery was brought to people's mind by Bin Li et al. Compared to other ZFB and FB,[21] the zinc-iodide has higher energy density, a discharge energy density of 167 $Wh^{-1}$. However, this system suffers the same problem as all ZFBs do: the zinc dendrite formation.[22] Zinc dendrite caused by the bad electrodeposition in the anode side will pierce into the separator surface and lead to a micro-short circuit.[23,24] In the meantime, the capacity will drop drastically and the reaction is no longer reversible. Besides, the kinetics and adsorption issue on cathode side has also been mentioned in the recent publications. Therefore, some methods to deal with these problems were proposed recently from Dr. Xianfeng Li's group.[25] They introduced a new type of self-healing membrane which could recover from the pierce and inhibit the micro-short circuit. Another method of doping Sn to the 3D current collector was also proposed from the same group. They achieved more than 100 cycles under 40 $mA/cm^2$ and 40 $mAh/cm^2$ in the zinc-bromine system. [26]

Meanwhile, the study of mechanism of zinc deposition in zinc batteries has attracted huge attention. In 2019, Jingxu Zheng from Dr. Archer's group from Cornell introduced the concept epitaxial growth to study zinc battery.[27] Since the epitaxial growth is basically an idea in semiconductor field, this publication drew a lot of attention once it

came out.[28–30] During the epitaxial electrodeposition process, a thin layer of zinc electrodeposit first forming a coherent of semi-coherent lattice interface with the electrode. This single crystalline layer of zinc will help the nucleation growth and thus forms a well deposited metal layer.[31] Graphene was applied in this article because of its low lattice mismatch of 7% compares to zinc.[32,33] Alignment of graphene is the key point for this method, a doctoral blade is used to dope graphene making it aligned on the 2D electrode surface.

In this chapter, we try to apply the epitaxial growth in the 3D flow battery system. The doping of graphene has been a huge issue in our case. 3D current collector has good porous structure which is important to flow performance. Although the method using doctoral blade can achieve alignment, it may block the hole and break down the porous structure. Several other ways were considered, the first one was the Langmuir-Blodgett Method from Kim Mun Sek et al. By applying Marangoni effect,[34,35] they can form aligned graphene on 3D surface. However, the graphene doped by this method is not stable due to weak attaching force. Another method was dipping method, this idea aims to use adsorption of graphene molecule.[36] In this case, the graphene is stable enough, but can't be aligned. With all these methods considered, we decided to use electrostatic force with electrospray. Electrospray is a method which adds an electric field to force liquid particles to move forward.[37,38] These particles will then be collected by a conductivity substrate, in this case 3D electrode and then stick to it. This a cheap and mature technique to be applied in the battery field. By using this method, we finally form an aligned, stable and good-sized layer of graphene on the 3D current collector

surface which will help the epitaxial growth of zinc in the anode.

Although being less important, we also try to deal with the cathode Iodine problem.[23,39] Active carbon, a well-known material for adsorption, is doped using the same method to further improve the system.[40] With the higher kinetics of cathode side and less adsorption of iodine, we can finally make a well-designed zinc-iodide system.

## 2. EXPERIMENTAL METHODS

### 2.1 Ink preparation

Due to different mechanisms in both side of the battery, we had different receipts for each side. The Anode side (Zinc side) consist of 4wt% of graphene and 96% of DI water while the cathode side content 1.5 wt% active carbon (AC), 0.5 wt% carbon black super P, 1 wt% Nafion dispersion (20 wt%, Ion power) and DI water. The Carbon black super P was added to improve the conductive and the Nafion dispersion worked as a binder to change the dispersivity.

### 2.2 Electrospray

The graphene ink for Anode was ultrasonicated for 60 minutes before use in order to while active carbon ink should be sonicated for 90 minutes to maintain well-dispersed. The solution was then switched to different 5 mL syringes with a needle (tube gauge 10, shell gauge 17). Ten psig of air was applied through the shell of the needle while the pump (Harvard Apparatus) pushing the syringes to spray the solution out. The current collector we used was 5mm x 7mm Carbon felt (C200, AvCarb, 6mm thick). The distance between needle and carbon felts varies from the solution. The AC solution was less homogeneous, thus the distance should be larger. AC particles would not

disperse easily under electric field, so the radius of carbon circle after electrospray was extremely small which could not fully cover the cathode surface. To avoid this, a larger distance was needed. The best distance was 18 cm after several tries. As for the graphene side, since graphene solution was homogenous enough, a distance of 10.5 cm was enough for the coverage of the surface. The best amount of solution for cathode side was 45 μL, and flow rate was set to 0.015 mL/min. For anode side, since the graphene may block the hole of carbon felt and broke down the porous structure, the amount of solution was strictly limited to 60 μL while the flow rate was 0.02 mL/min.

**2.3 Single cell testing**

Unlike the vanadium flow battery, the Zinc Iodine flow battery was a single flow system, the fluid in the anode side (Zinc) would circulate as normal while the liquid for the cathode side (Iodide) would not. The electrolyte used for both sides was a mixture of 3M $ZnBr_2$ (Alfa Aesar, 99.0%) and 6M KI (Sigma-Aldrich, 99.9%). The catholyte would be pre-pumped into the cathode side and then blocked with pipes, then 40 mL of electrolyte would be circulated as anolyte. The reason for this change is that the generation of Iodine is inevitable, since the Iodine was in solid state the flow of the electrolyte would result in blockage of tubing. The electrode we used was C200 (AvCarb, 6mm thick) and separator was Nafion 115 (Ion power). The charging settings were: 15 minutes and 3A and discharge settings were: 0.2 V and 3A. For both charge and discharge process the current density would reach 100 $mA/cm^2$ and areal capacity would reach 25 $mAh/cm^2$.

**2.4 Materials Characterization**

Both the Graphene treated and AC treated graphite felts were characterized by different kinds of analytical techniques. The XRD (Rigaku SmartLab X-Ray Diffractometer) was used to examine the carbon morphology. Raman spectroscopy (Renishaw InVia Confocal Raman microscope, 785nm laser) was applied to detect the carbon crystallinity and morphology. SEM (Zeiss Gemini 500 Scanning Electron Microscope) was used to observe the structure of the carbon fiber before and after the electrodeposition.

### 2.5 Electrochemical Measurement

*Cyclic Voltammetry*

Due to the high resistance of flow battery, we used the coin cell testing instead of the three-probe tests. We applied the same electrode, separator and electrolyte into the coin cell system to examine the electrochemical kinetics of the Iodide side. An electrolyte consisting of 0.05M $ZnI_2$ was used for all testing with electrode of AC-doped Carbon felt. Cyclic voltammetry (CV) was performed on the electrolytes at rates of 5, 10, 15, 20, 25, 30 and 50 mV/s.

## 3. RESULTS AND DISCUSSION

The goal for these treatments is to find a way to better design the Zinc Iodide flow battery (ZIFB) using the electrospray technique to modify the electrode. Before that, we should first identify the key factor for the Zinc Iodide flow battery. Just like all other Zinc-Based flow battery, ZIFB also suffers from the severe anode problem: the Zinc dendrite formation. Dead Zinc with huge amount of dendrite will not only reduce the capacity and coulombic efficiency, but also pierce into the Nafion membrane causing

micro-short circuit. Although the dendrite has been the main problem for Zinc-based flow battery, the cathode had found to have huge influence on the ZIFB performance in the experiments. The Iodine generated in the cathode side would precipitate on the surface of separator which would lead to extremely low ion conductivity and bad cycling reversibility. Therefore, solving these two issues have been the key point for improving the performance of ZIFB.

To solve the previous problems, carbon materials were selected to improve the interfacial properties of current collectors. The electrospray was chosen as the main technique to dope it. SEM was used to analyze the treated felts especially for the graphene treated one, as shown in Figure 3.1.

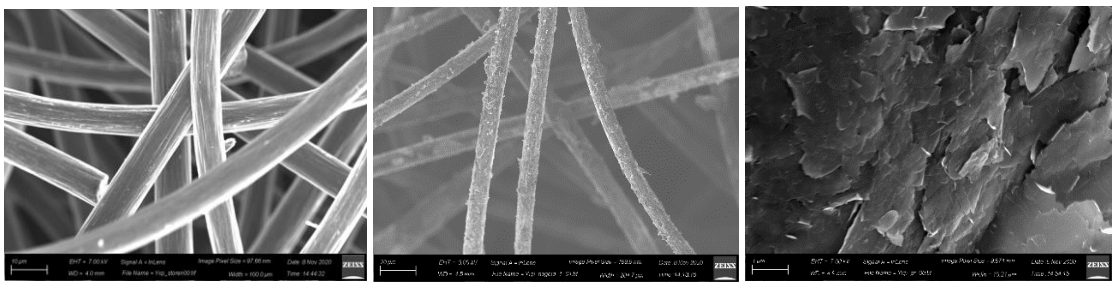

**Figure 3.1. SEM images of (A) pristine CF (B) Gr doped CF under 200μm scale (C) Layer structure of Gr on CF under 10μm scale.**

As it showed in Figure 3.1B, the sprayed felts were covered by graphene uniformly, while maintaining the porous structure. And in lower scale of 10 nm in Figure 3.1C, we could see the special layered align pattern of graphene. These SEM images indicated the good feasibility of electrospray to dope aligned graphene stably on the carbon felt surface. Electrodeposition tests of Zinc were done for both baseline and graphene treated felts. SEM images of Figure 3.2 showed a clear difference between the treated and untreated felts. Figure 3.2A and Figure 3.2B showed the pristine carbon after

electrodeposition, though the carbon felt was in 3D structure, the newly generated metal was clinging to surface and aggregated. This would lead to severe dendrite formation

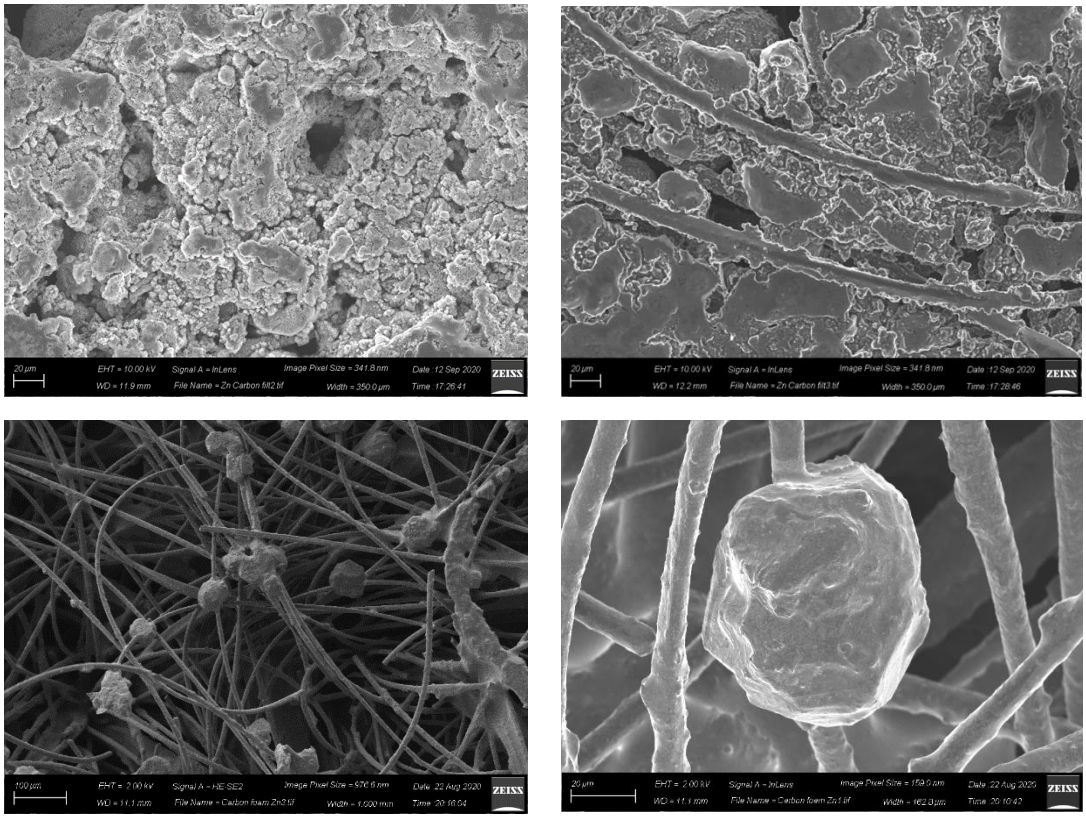

**Figure 3.2. SEM images after electrodeposition. (A) (B) Images of pristine CF under Zinc electrodeposition. (C)(D) Images of Zinc deposition on Gr treated CF.**

causing capacity decay and cycling issue. However, for treated cases, Zinc metal would grow along the carbon fiber, making full use of the 3D structure of carbon felt without aggregating on the anode surface (Figure 3.2C, 3.2D). A series of tests were taken to better understand how much graphene treatment contributed to the improvement of the performance of each single cell test. This included control tests, 1 micron thickness of graphene and 5 micron thickness under different current density of 40 mA/cm$^2$ and 80 mA/cm$^2$. The result of 40 mA/cm$^2$ was showed in Figure 3.3. In this case, the charging time was set to 15 minutes and the areal capacity was 10 mAh/cm$^2$. The Graphene

treated carbon felt (GTCF) showed a great improvement compares to the pristine one, the control group could only maintain high coulombic efficiency (over 95%) for about 40 cycles, but graphene treated one could achieve a CE of over 99% for over 260 cycles

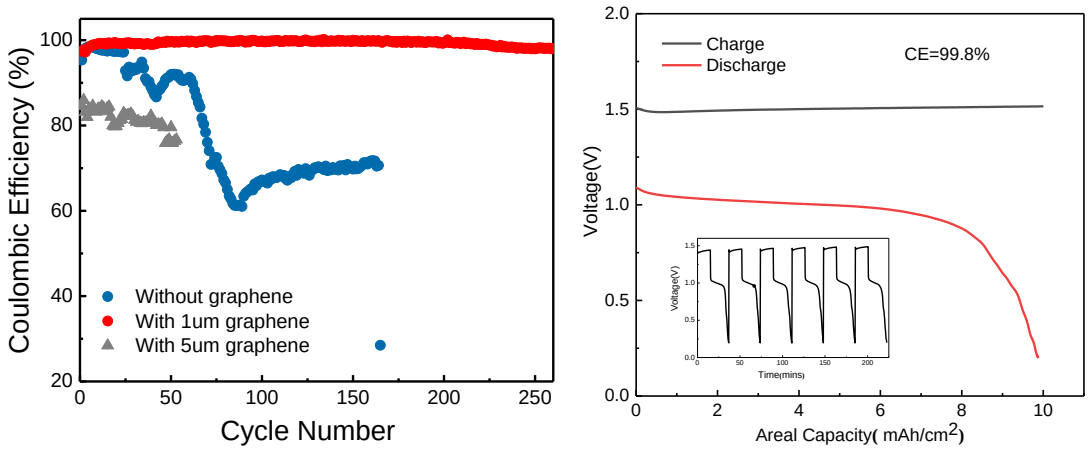


**Figure 3.3. Comparison of cycling performance with difference amount of Gr under current density of 40 mA/cm$^2$. (A) Coulombic efficiency (B) Capacity-Voltage curve.**

and maintain acceptable overpotential during that time. The high graphene amount case was also been tested. With 5 microns thickness of graphene doping on the surface, the battery even couldn't reach 99% efficiency. The main reason for that was the bad porosity of felts after being heavily doped. Since graphene solution turned to have the nature to aggregate, the larger the amount doped, the higher the possibility for the pores to be blocked. As a flow system, this congestion could be a huge problem. After testing the flow performance of different doping amount of GTCF, the best thickness was 1 micron. Based on this result, we continued to use the same amount and applied this GTCF to 80 mA/cm2 and 13.3 mAh/cm2 (Figure 3.4). Although we doubled the current density, the battery using GECF could still reach 150 cycles at a coulombic efficiency of over 99%, however, under such severe condition, the control group died at around

20 cycles generating a lot of dead Zinc and thus causing high overpotential and low

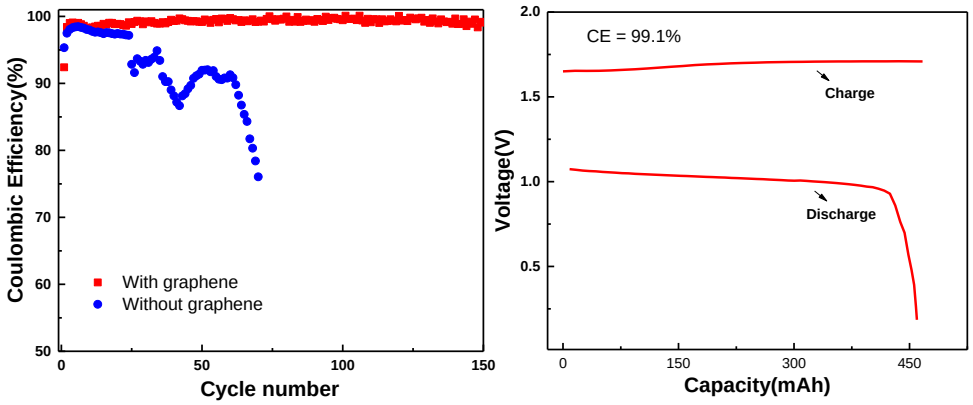


**Figure 3.4. Comparison of cycling performance with difference amount of Gr under current density of 80 mA/cm$^2$. (A) Coulombic efficiency (B) Capacity-Voltage curve.**

efficiency. These results demonstrated that we could achieved good performance of ZIFB using graphene, attributed to the application of aligned graphene using electrospray thus led to a good epitaxial growth of Zinc in the anode side.

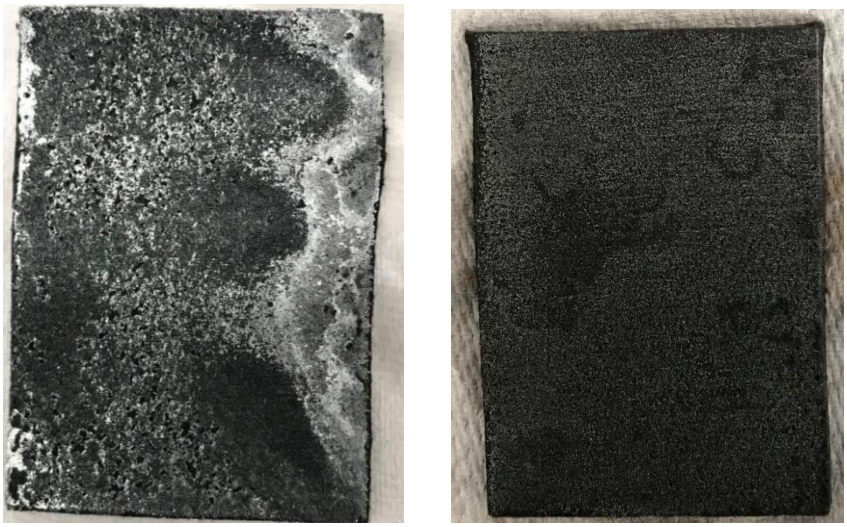

**Figure 3.5. Carbon felt morphology after cycling. (A) Pristine CF after cycling for 40 cycles. (B) Gr doped CF after cycling for 150 cycles.**

The carbon felts were taken out from the flow cell after the experiments, showed in Figure 3.5. The Figure 3.5A was the anode of control group while Figure 3.5B belongs

to the GTCF. We could tell that there was an obvious difference between the two felts which indicates the ability for this method to stabilize the electrodeposition process. XRD was done to both felts, as showed in Figure 3.6. The figure demonstrated that there were inevitable side reactions happen during the process. Hydrogen ion would accept 2 electron forming Hydrogen gas as the Zinc dendrite generating. The formation of ZnO represents this process, for the control group (Figure 3.6B), the peak of Zn0 was pretty strong while in the graphene-doped case (Figure 3.6A), ZnO peak disappeared indicating this side reaction was larger prevented. Raman analysis

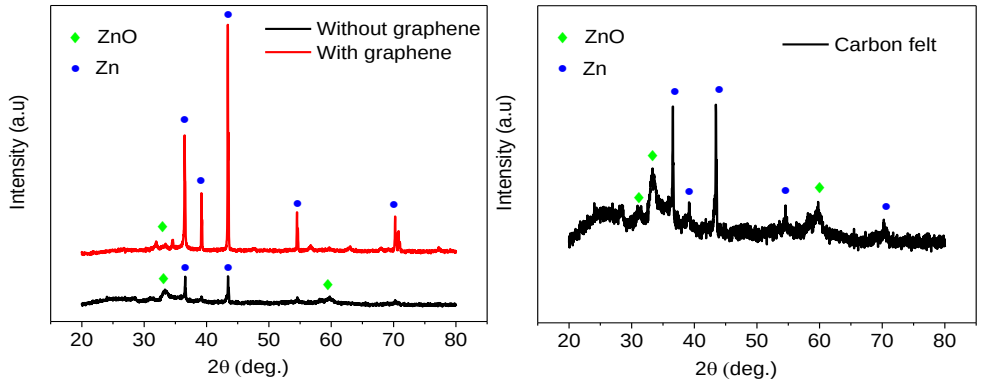


**Figure 3.6. (A) Comparison of CF and GTCF on XRD. (B) XRD for Pristine CF**

was applied with a wavelength of 532 nm. The Disorder Band (D Band) and the Graphitic Band (G band) were showed below. The relative intensity ratio of these two peaks indicates the degree of crystallinity of carbon network. The $I_D/I_G$ for Doctor-blade-type was 0.3778 while the ratio for electrospray case was 0.1966. This ratio difference showed an apparent increase in the fraction of crystalline carbon in the electrospray one compared to doctor-blade case used in 2D materials. This indicated

that with the use of electrostatic force, the graphene on the surface could be more aligned thus had less defects. Therefore, in conclusion, the graphene doped by electrospray can easily form an aligned structure of graphene which will lead to Zinc

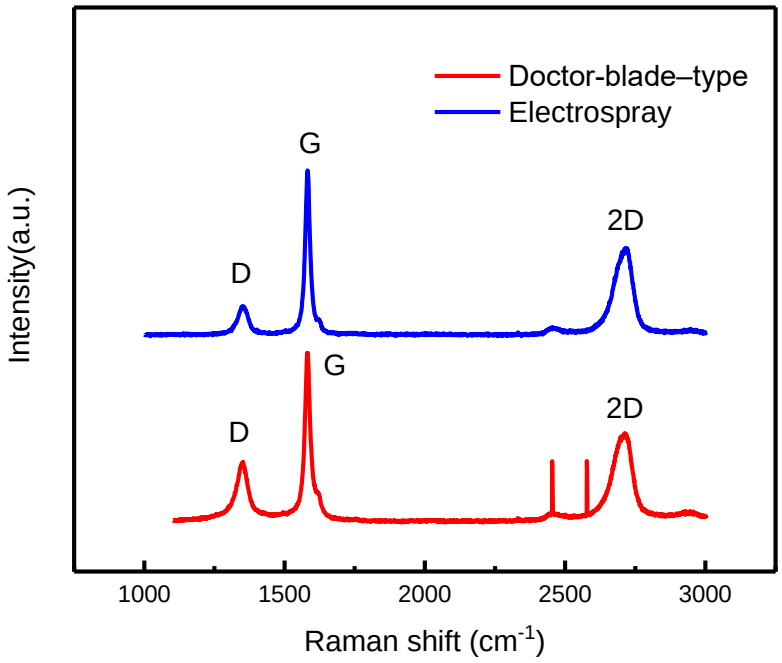


**Figure 3.7. Raman spectroscopy of Doctoral-blade-type graphene and Electrospray graphene on Si wafer.**

epitaxial growth along the carbon fiber. This process will then help reduce the dendrite formation and stabilize the electrodeposition. The electrosprayed graphene has less defects and will also help reduce the side reaction (Figure 3.7).

While studying the anode mechanism, we found out that the cathode side also had great problem. As it showed in the Figure 3.8 and Figure 3.9. The Iodine generated during

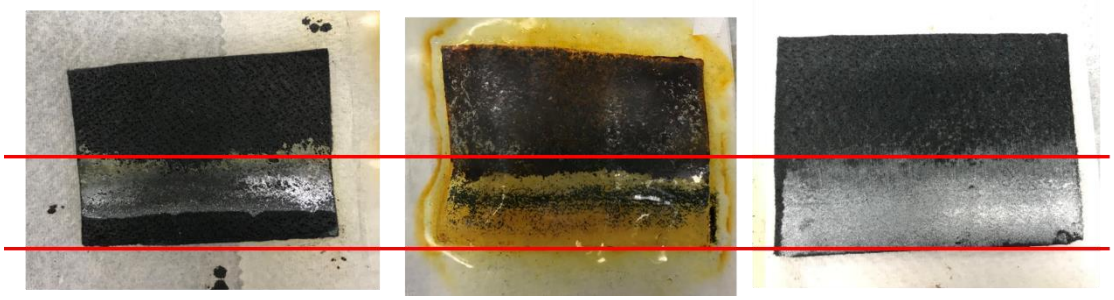

**Figure 3.8. (A) Cathode after 40 cycles under current density of 40 mA/cm$^2$. (B) Separator after cycling for 40 cycles. (C) Anode for the same battery.**

the reaction would more likely to aggregate on the Nafion instead of the pristine carbon felt. This layer of Iodine would largely decrease the ion conductivity and increase the system resistance. Since we were already using extremely high current in this case, the diffusion of the Potassium ion would be the constrain factor of the system. Therefore, this formation of Iodine layer could be a deadly issue to the ZIFB. In the Figure 3.9A case, the Iodine even covered the Nafion completely and the same battery died in several cycles. The key point to deal with this problem is to localize the $I^-$, $I_3^-$ and $I_2$ at

**Figure 3.9. (A) Nafion 115 fully covered by Iodine after cycles. (B) The Nafion 115 after 150 cycles using GTCF.**

the current collector surface to minimize the blocking effect as well as increase the

reaction kinetics (Figure 3.11). Hence, we choose several different adsorption ability materials to prove our assumptions. We tried Carbon nanotube (CNT), graphene, and active carbon (AC). The theoretical adsorption ability was: graphene < Carbon nanotube < Carbon felt < Active carbon. However, the result we have now is not consistent with our assumption showed in Figure 3.10. This is because we ignore the electro-conductivity influence on the reaction process. Although AC has strong adsorption ability, terrible electro-conductivity. As a result of this, we involved the Super P to modify the electro-conductivity.

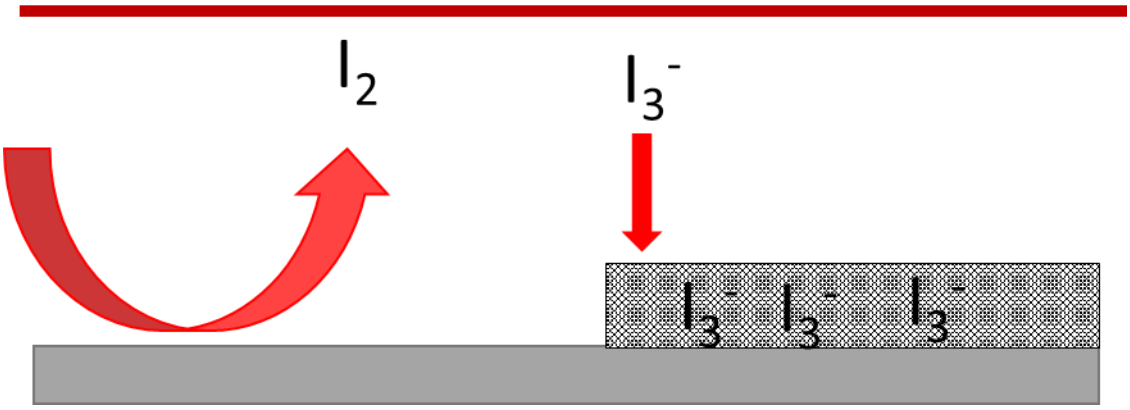


**Figure 3.11 Schematic of iodine and iodide adsorption.**

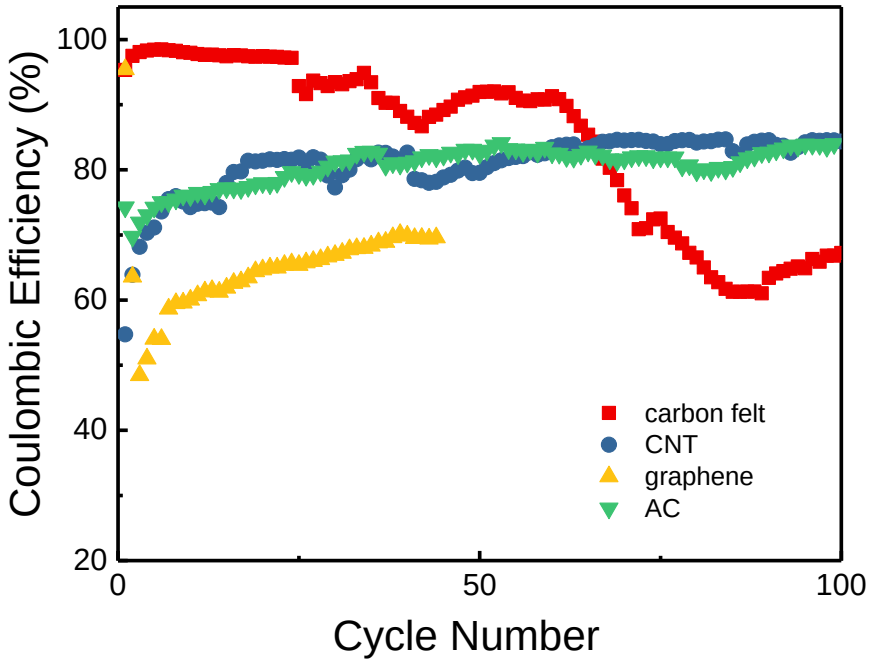


**Figure 3.10 Comparison of different carbon materials doped onto the cathode surface: CNT, Gr, AC.**

CV tests had been done to study the kinetics in the cathode side, we tried a scan rate of 5 mV/s to 50 mV/s showed in Figure 3.12. The Figure 3.12A was the data for AC coated

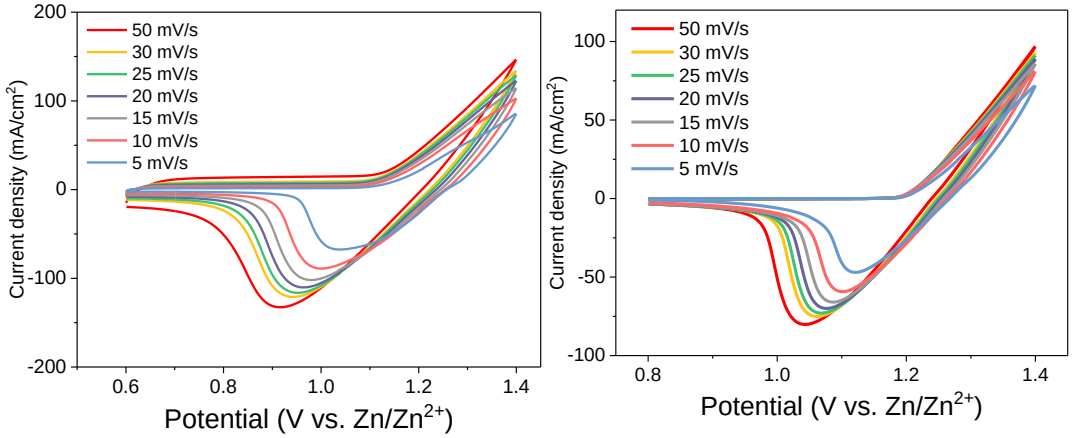


**Figure 3.12. CV plot with scan rate of 5mV/s TO 50mV/s. (A) Plot for AC treated CF (B) Plot for pristine CF.**

carbon felt while the Figure 3.12B was the one for control group. We could figure out that the cathodic peak after doping the AC dropped from 1.1V to 0.95V and the maximum peak height was much greater than the control which suggests that this AC

treated carbon felt had more favorable reaction kinetics. The AC treated carbon felt also had higher current density under the same voltage as the control group indicated a drop in the overpotential of the reaction and proofed that the AC doped carbon felt could maintain electroactive situation under high current environment. We could have a better view of this kinetics change in the scan rate of 25 mV/s showed in Figure 3.13. A rate capability test was done to further prove this idea (Figure 3.14). As the current density grew, the performance of battery went done in the control group, however, after doping the AC the efficiency maintained quite well even under a current density of 100 mA/cm2. All these effects are attributed to the adsorption ability of AC, the Iodide

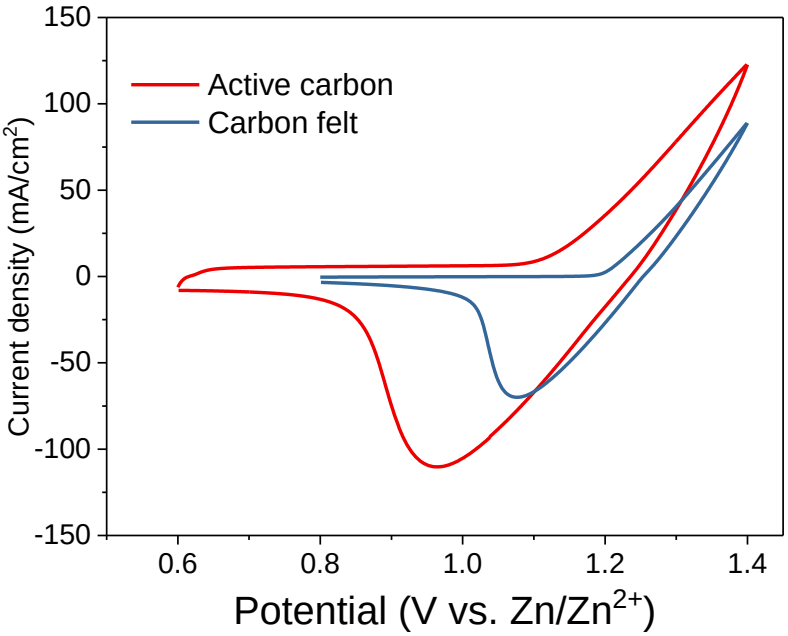


**Figure 3.13. CV plot under scan rate of 25mV/s**

and Iodine would be absorbed onto the surface of carbon felt avoiding the precipitation on the separator thus reduce the blocking effect. Meanwhile, as the result suggested, the AC would improve the kinetics as well, offering more active sites for the reaction. Other analysis on the peak current and cathodic slope had been done to

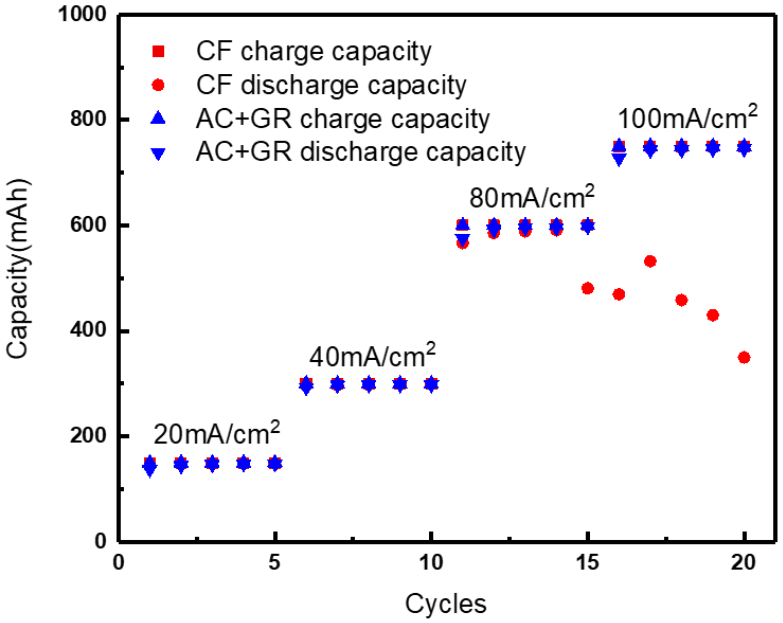


**Figure 3.14 Rate capability test of Both treated case and pristine CF. The current density ranged from 20 mA/cm$^2$ to 100 mA/cm$^2$.**

further prove the previous idea in Figure 3.15. The Figure 3.15A showed the relationship between the root of scan rate and the peak current. We could have a clear view that the current with active carbon was higher than the control group. In the Figure 3.15 B, the cathodic and Anodic slope were presented. Active carbon treated one for both cases had significant improvement. All these phenomenon indicated the faster

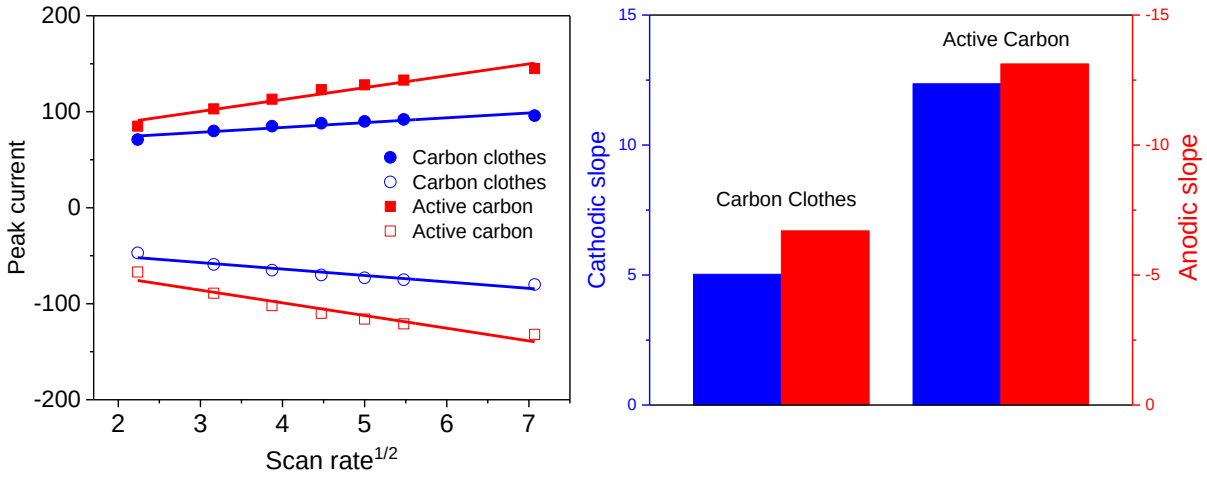


**Figure 3.15. (A) Scan rate-peak current plot. (B) Cathodic slope and anodic slop**

kinetics of AC treated case. Single cell testing had proved the feasibility of applying both modifications. In the Figure 3.16, we applied an extremely high current density:

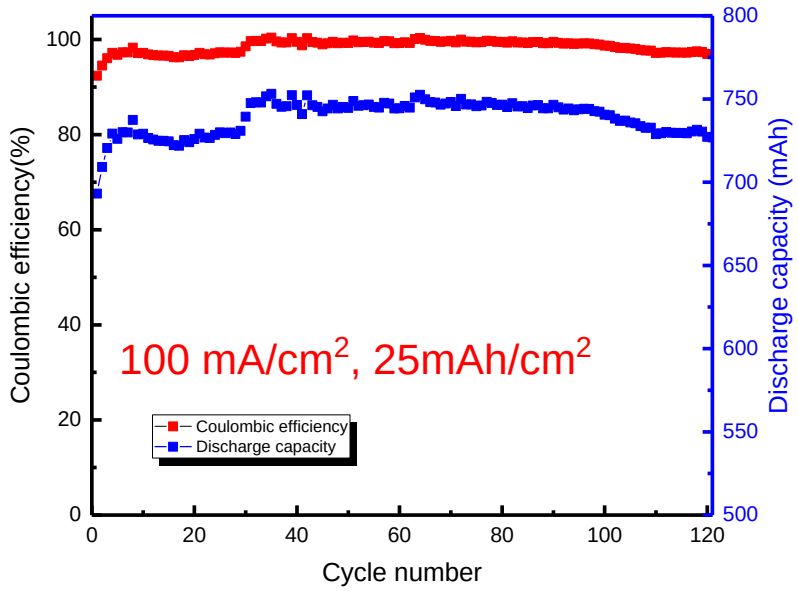


**Figure 3.16. The cycling performance of both treated case under current density of 100 mA/cm$^2$ and areal capacity of 25 mAh/cm$^2$.**

100 mA/cm$^2$ and a decent areal capacity of 25mAh/cm$^2$. The result was astonishing, the Coulombic efficiency reached over 99% and lasted for over 120 cycles while the

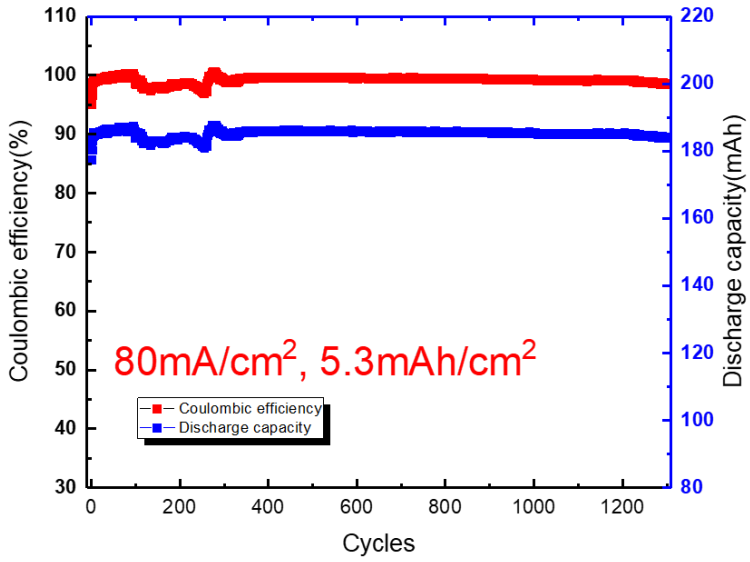


**Figure 3.17. Cycling test of both treated case under current density of 80 mA/cm$^2$ and 5.3 mAh/cm$^2$.**

capacity maintained to about 740 mAh. A lower current density and areal capacity were tried to test the battery's reversibility (Figure 3.17). The current density was set to 80 mA/cm$^2$ while the areal capacity was 5.3 mAh/cm$^2$. The battery maintained 99% Coulombic efficiency and high discharge capacity for over 1300 cycles, totally of 315 hours. Other control tests were done to discuss the effect of GTCF, AC treated CF pristine CF (Figure 3.18). In the same condition, the pristine CF could only maintain good electrodeposition for less than 10 cycles, the GTCF on anode could last for 35 cycles, while the CF with AC on cathode could maintain 60% of efficiency. However, for the both treated case, the Coulombic efficiency maintained over 99% for 120 cycles

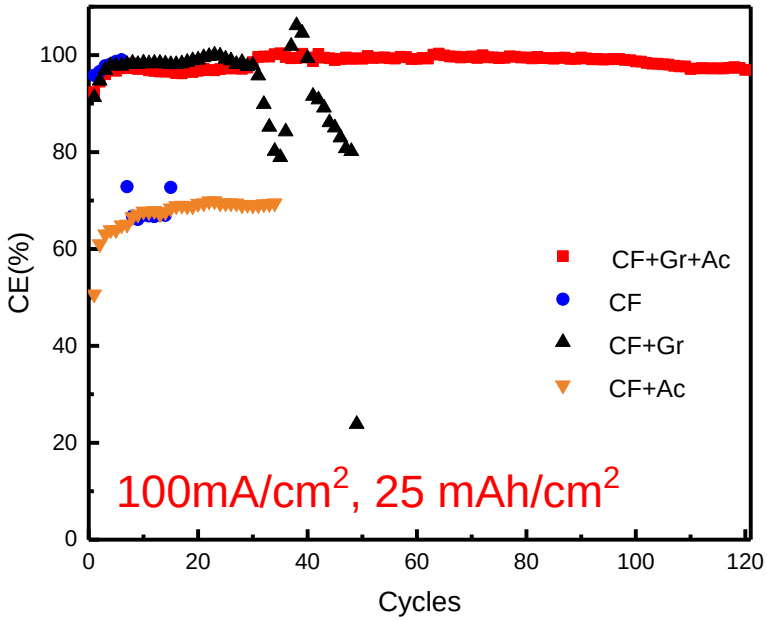


**Figure 3.18. Comparison between both treated, only anode Gr treated, only cathode AC treated and control group.**

indicating a great electrodeposition improvement. The separator from this battery was taken out (Figure 3.8B), compared to the untreated case in Figure 3.8A, it was significantly cleaner without Iodine on the surface. This result was consisted to our assumption, the AC doped on the surface could largely improve the reaction kinetics by absorbing the $I_3^-$ and $I^-$ onto to surface while in the meantime, help absorb the remaining solid-state Iodine avoiding the reduce of membrane ion conductivity.

## 4. CONCLUSION

The GTCF using electrospray had proven to achieve epitaxial growth on the 3D current collector surface. The electrostatic force helped the graphene to form an aligned layer on the surface thus achieving uniform Zinc electrodeposition and inhibited the formation of Zinc dendrite. While in the cathode side, the We applied AC to the CF

changing the reaction kinetics and absorbed the remaining Iodine to avoid blocking effect. The good performance in the single cell testing had further proved our assumption, we reached an areal capacity of 25 mAh/cm$^2$ under current density of 100 mA/cm$^2$ for over 120 cycles with 99% of coulombic efficiency which was quite promising.

***Reference***


1. Turner, J. A. A Realizable Renewable Energy Future. 285, 687–690 (1999).

2. Yang, Z. et al. Electrochemical Energy Storage for Green Grid. 3577–3613 (2011).

3. Dunn, B., Kamath, H. & Tarascon, J. M. Electrical energy storage for the grid: A battery of choices. Science (80-. ). 334, 928–935 (2011).

4. Wang, W. et al. Recent progress in redox flow battery research and development. Adv. Funct. Mater. 23, 970–986 (2013).

5. Zhang, H. Progress and perspectives of flow battery technologies. Curr. Opin. Electrochem. 18, 123–125 (2019).

6. Rychcik, M. & Skyllas-Kazacos, M. Characteristics of a new all-vanadium redox flow battery. J. Power Sources 22, 59–67 (1988).

7. Yuan, Z. et al. Advanced Materials for Zinc-Based Flow Battery: Development and Challenge. Adv. Mater. 31, 1–27 (2019).

8. Gong, K. et al. A zinc-iron redox-flow battery under $100 per kW h of system capital cost. Energy Environ. Sci. 8, 2941–2945 (2015).

9. Yang, B., Hoober-Burkhardt, L., Wang, F., Surya Prakash, G. K. & Narayanan, S.

R. An Inexpensive Aqueous Flow Battery for Large-Scale Electrical Energy Storage Based on Water-Soluble Organic Redox Couples. J. Electrochem. Soc. 161, A1371–A1380 (2014).

10. Braff, W. A., Bazant, M. Z. & Buie, C. R. Membrane-less hydrogen bromine flow battery. Nat. Commun. 4, (2013).

11. Zhang, J. et al. An all-aqueous redox flow battery with unprecedented energy density. Energy Environ. Sci. 11, 2010–2015 (2018).

12. Skyllas-Kazacos, M., Chakrabarti, M. H., Hajimolana, S. A., Mjalli, F. S. & Saleem, M. Progress in Flow Battery Research and Development. J. Electrochem. Soc. 158, R55 (2011).

13. Parasuraman, A., Lim, T. M., Menictas, C. & Skyllas-Kazacos, M. Review of material research and development for vanadium redox flow battery applications. Electrochim. Acta 101, 27–40 (2013).

14. Chakrabarti, M. H., Hajimolana, S. A., Mjalli, F. S., Saleem, M. & Mustafa, I. Redox Flow Battery for Energy Storage. Arab. J. Sci. Eng. 38, 723–739 (2013).

15. Luo, Q. et al. Capacity decay and remediation of nafion-based all-vanadium redox flow batteries. ChemSusChem 6, 268–274 (2013).

16. Prifti, H., Parasuraman, A., Winardi, S., Lim, T. M. & Skyllas-Kazacos, M. Membranes for redox flow battery applications. Membranes (Basel). 2, 275–306 (2012).

17. Cheng, J. et al. Preliminary study of single flow zinc-nickel battery. Electrochem. commun. 9, 2639–2642 (2007).

18. Leung, P. K., Ponce-De-León, C., Low, C. T. J., Shah, A. A. & Walsh, F. C.

Characterization of a zinc-cerium flow battery. J. Power Sources 196, 5174–5185 (2011).

19. Leung, P. K., Ponce De León, C. & Walsh, F. C. An undivided zinc-cerium redox flow battery operating at room temperature (295 K). Electrochem. commun. 13, 770–773 (2011).

20. Society, T. E. Zinc - Bromine Secondary Battery Zinc-Bromine Secondary Battery. (1977).

21. Li, B. et al. Ambipolar zinc-polyiodide electrolyte for a high-energy density aqueous redox flow battery. Nat. Commun. 6, (2015).

22. Khor, A. et al. Review of zinc-based hybrid flow batteries: From fundamentals to applications. Mater. Today Energy 8, 80–108 (2018).

23. Li, Z., Weng, G., Zou, Q., Cong, G. & Lu, Y. C. A high-energy and low-cost polysulfide/iodide redox flow battery. Nano Energy 30, 283–292 (2016).

24. Xie, C., Liu, Y., Lu, W., Zhang, H. & Li, X. Highly stable zinc-iodine single flow batteries with super high energy density for stationary energy storage. Energy Environ. Sci. 12, 1834–1839 (2019).

25. Xie, C., Zhang, H., Xu, W., Wang, W. & Li, X. A Long Cycle Life, Self-Healing Zinc-Iodine Flow Battery with High Power Density. Angew. Chemie 130, 11341–11346 (2018).

26. Yin, Y. et al. Dendrite-Free Zinc Deposition Induced by Tin-Modified Multifunctional 3D Host for Stable Zinc-Based Flow Battery. Adv. Mater. 32, 1–8 (2020).

27. Zheng, J. et al. Reversible epitaxial electrodeposition of metals in battery anodes. 648, 645–648 (2019).

28. Copel, M., Kaxiras, E., Tromp, M. & Stranski-krastanov, T. Surfactants in Epitaxial Growth. Phys. Rev. Lett. 63, 632–635 (1995).

29. Zhu, F. F. et al. Epitaxial growth of two-dimensional stanene. Nat. Mater. 14, 1020–1025 (2015).

30. Tan, C., Chen, J., Wu, X. J. & Zhang, H. Epitaxial growth of hybrid nanostructures. Nat. Rev. Mater. 3, 1–13 (2018).

31. Chambers, S. A. Epitaxial growth and properties of thin film oxides. Surf. Sci. Rep. 39, 105–180 (2000).

32. Srikant, V., Speck, J. S. & Clarke, D. R. Mosaic structure in epitaxial thin films having large lattice mismatch. J. Appl. Phys. 82, 4286–4295 (1997).

33. Zheleva, T., Jagannadham, K. & Narayan, J. Epitaxial growth in large-lattice-mismatch systems. J. Appl. Phys. 75, 860–871 (1994).

34. Kim, M. S., Ma, L., Choudhury, S. & Archer, L. A. Multifunctional Separator Coatings for High-Performance Lithium–Sulfur Batteries. Adv. Mater. Interfaces 3, (2016).

35. Kim, M. S. et al. Langmuir–Blodgett artificial solid-electrolyte interphases for practical lithium metal batteries. Nat. Energy 3, 889–898 (2018).

36. Park, S. & Kim, H. Fabrication of nitrogen-doped graphite felts as positive electrodes using polypyrrole as a coating agent in vanadium redox flow batteries. J. Mater. Chem. A 3, 12276–12283 (2015).

37. Shah, A. B., Zhou, X., Brezovec, P., Markiewicz, D. & Joo, Y. L. Conductive Membrane Coatings for High-Rate Vanadium Redox Flow Batteries. ACS Omega 3, 1856–1863 (2018).

38. Halim, W. et al. Directly deposited binder-free sulfur electrode enabled by air-controlled electrospray process. ACS Appl. Energy Mater. 2, 678–686 (2019).

39. Ramette, R. W. & Sandford, R. W. Thermodynamics of Iodine Solubility and Triiodide Ion Formation in Water and in Deuterium Oxide. J. Am. Chem. Soc. 87, 5001–5005 (1965).

40. Li, Z. & Lu, Y. C. Material Design of Aqueous Redox Flow Batteries: Fundamental Challenges and Mitigation Strategies. Adv. Mater. 32, 1–30 (2020).

# CHAPTER 5

# FUTURE WORK

Due to an increasing global concern regarding to the clean energy and the shortage of fossil fuel storage, the need for clean, cheap and efficient renewable energy has been increasing drastically. Designed for large scale energy uses, flow battery come into our sight due to its high efficiency, high capacity, high safety and flexible design. Right now, the most common type of flow battery: vanadium flow battery has been widely-used for large scale facilities and also been used as the backup energy storage for hospitals.

The key factor for flow batteries varies from different types. In this thesis, we mainly discussed about vanadium flow battery and zinc iodide flow battery. We doped functional groups to electrode using APS to solve the reaction kinetics issue for vanadium system. While finishing the vanadium project, some modifications to the membrane were also applied. Carbon material like CNT and graphene were sprayed onto the surface to increase conductivity while in the meantime, reduce the crossover. We could see huge capacity and reversibility improvement for these two modifications. For the zinc iodide battery, the key point was the electrodeposition. Graphene and active carbon were doped to electrode surface in order to control the electrodeposition. The epitaxial growth of zinc was achieved which led to 120 cycles for high current density and areal capacity.

For future work, it would be worthwhile to consider doping nano copper onto the electrode surface for vanadium flow battery. Instead of incorporating sulfonic

functional groups, the nano copper has proved to have better catalytic effect on the reaction. With the use of electrospray technique, we can easily achieve good shape of nano copper on the surface without blocking the porous structure of electrode.

Another future project to be explored is the new system of zinc vanadium flow battery. With the reaction of zinc ion to zinc and V(IV) to V(V), high voltage is expected. If we can solve the problem of crossover by doing modification to the separator, this battery can be a good replacement for traditional vanadium redox flow battery.